Thermo-mechanical Processing of API-X60 Grade Pipe Line Steel.

A THESIS IS SUBMITTED IN PARTIAL FULFILMENT

OF THE REQUIREMENT FOR THE AWARD OF THE DEGREE OF

Master in Technology

In

Mechanical Engineering.

Submitted By:

DIPESH KUMAR MISHRA

ROLL NO: 212MM2421

(Specialization: Steel Technology)

Department of Metallurgical and Materials Engineering

National Institute of Technology

Rourkela-769008.

Thermo-mechanical Processing of API-X60 Grade Pipe Line Steel.

A THESIS IS SUBMITTED IN PARTIAL FULFILMENT

OF THE REQUIREMENT FOR THE AWARD OF THE DEGREE OF

Master in Technology

In

Mechanical Engineering.

Submitted By:

DIPESH KUMAR MISHRA

ROLL NO: 212MM2421

(Specialization: Steel Technology)

UNDER GUIDENCE OF:

Dr.S.K.SAHOO

(ASSISTANT PROFESSOR)

Department of Metallurgical

& Material Engg.

NIT-ROURKELA-769008

Dr.S.G.CHOWDHURY

(Sr.Principal Scientist)

MST, Department

NML, JAMESHEDPUR

JARKHAND-831007

May -2014.

NATIONAL INSTITUTE OF TECHNOLGY, ROURKELA

ORISSA-769008

CERTIFICATE

*This is certify that the thesis entitled "**Thermo-mechanical Processing of API-X60 grade Pipe line Steel**" has submitted by "**Mr.Dipesh Kumar Mishra**" in partial fulfilment of the requirement for the degree of "**Master in Technology**" in **Mechanical Engineering** with specialization in "**Steel Technology**", is a bonafide work carried out by him under supervision and guidance. In our opinion, the work fulfils for which it is being submitted.*

To the best of our knowledge, the matter embodied in the thesis has not been submitted to any other University / Institute for the award of any Degree or Diploma.

Dr. S.K.SAHOO.
Assistant Professor
Department of Material
& Metallurgical Engg.
NIT, ROURKELA-769008
Date:
Place:

Dr.S.G.CHOWDHURY
(Sr.Principal Scientist)
MST, Department
NML, JAMESHEDPUR
JARKHAND-831007
Date:
Place:

MAY-2014

Acknowledgments

I take this opportunity to express my deep indebtedness to Dr S.K.Sahoo(Assitant Professor) Department of Material and Metallurgical Engineering, NIT-Rourkela and V.Rajnikant(Scientist) National Metallurgical Laboratory,Jameshedpur for his valuable guidance and supervision towards the completion of my M.Tech thesis work. His incessant encouragement and suggestion was invaluable .I feel fortunate for support, involvement and well wishes of my mentors and this is virtually impossible to express them in words.

I express my sincere gratitude and indebtedness to Dr.S.K.Sarangi, Director NIT, Rourkela and Dr S.Srikant Director CSIR NML, Jameshedpur for having permitted me to carry out this project work.I would like to give thank to Dr.Sandip Gosh Choudhary (Senior Principal Scientist at NML) for extending their support and suggestion and give chance to access all the facilities of the laboratory,required for my research work.
I do not want to overlook the help that has been rendered to me by all well wishes from the core of my heart like to give thanks to all .I would like to single out some people who have been especially instrumental, directly or indirectly, in completing this piece of work who are Sanjay, Rao Sir, Ranjit and Raman ji deserve the special position for my life and also for completing to my thesis in visible and invisible way.

Finally I most gratefully acknowledgement to my parents for staying in my heart and their continuous guidance in each step of my life ,without which it would have been impossible for me to reach this stage.I am also thankful to all my Hall-8 and Magnesium Hostel friend with whom ,I had a memorable time during the entire course period.

Date: (Dipesh Mi

CONTENTS

LIST OF FIGURES

LIST OF TABLES

ABSTRACT

The development of high strength pipeline steel grades is major concern for a large number of steel manufacturers. The mechanical properties of API high strength steel can be remarkably improved through proper alloy design and appropriate thermo-mechanical processing that can refine and homogenize the final microstructure. The API X 60 grades conventionally is of ferrite-pearlite microstructure. The high strength API X80 grades is of acicular ferrite/Bainite microstructure. The present objective is to obtain the acicular ferrite/Bainite micro structural constituents in the given API-X60 grade pipeline steel by thermo-mechanical processing. The thermo mechanical process involves heating to austenitization at 1200^0C for 20 min followed by deformation at temperatures of 900^0C, 1000^0C & 1100^0C for different strain levels at 0.4,0.8 &1.2 with constant strain rate of 2 sec^{-1} in a deformation dilatometer. After hot deformation, the specimens were quenched in water to retain the state of hot deformed austenite. The metallographic and EBSD results reveal the formations of Acicular Ferrite in case of sample deformed at 900^0C which is reported to have good combinations of strength & toughness and there is formation of bainite and martensite at 1000^0Cand 1100^0C deformed samples respectively. The critical point of stress and strain regarding to occurrences of DRX (Dynamic Recrystallisation) at each temperature was calculated from the flow curves based on the order of stress-strain curve and also the fraction of recrystallised volume in the sample which basically deformed at high temperature is calculated.

CHAPTER NO: 1

INTRODUCTION

INTRODUCTION

The improvement of high quality pipe line steel is a real sympathy towards countless producers. The primary capacity of the pipe line steel is to enhance the transport effectiveness with higher weight and transmission rate for long separations. Longitudinally welded huge width pipeline are utilized for the transportations of oil and gas in light of the fact that it offers the high well being in pipeline operations and speak to the financial results. The real test to the pipeline maker is to enhance the properties to oppose under diverse discriminating conditions, for example, under high profundity more than 2000m in seaward area or convey destructive liquids which are demonstrated in fig (1.1).Hence, pipeline steel must have high quality and sturdiness values at greatly low temperature. These properties might be accomplished in programming interface grade micro alloyed steels. Microstructure of these steels for the most part comprises of ultra-fine grains with some portion of Baninite and Martensite constituents [1].

Figure (1.1): Network of Pipe line distributions in various countries at high depth. [2]

In general, the pipelines are made of micro alloyed steel having properties commensurate with the standards of the American Petroleum Institute (API). These steels generally are intended for applications with dominant consideration of the efficiency to cost ratio with profitable weight reduction in wall thickness. These steels must have improved tensile strength, yield to tensile strength ratio, elongation, weld ability, susceptibility to hydrogen induced cracking particularly for sour service applications, low temperature impact toughness and ductile to brittle transition temperature [3]. These properties are basically acquired by the suitable additions of different micro alloying components [3,4],for example ,Ti,B,P,N,S,Mn,V,Nb and so forth, through controlled thermo-mechanical processing and cooling rates. Micro alloyed or high strength low alloy steel (HSLA) steel constitute an essential class assessed to be around 12% of aggregate world steel creation. They are utilized as a part of each real steel market area in different part of the world and their advancement has assumed a critical role in the extension of certain key industry, for example oil and gas extraction, developments and transportations.

The API steels are characterized on the basis of their leading micro alloying constituent and their effect during thermo-mechanical process. The thermo-mechanical processing is a nonexclusive term portrayed as plastic deformation of steel throughout high temperature medication to enhance the mechanical properties by fitting configuration of hot moving methodology courses which are indicated in fig in fig (1.2).

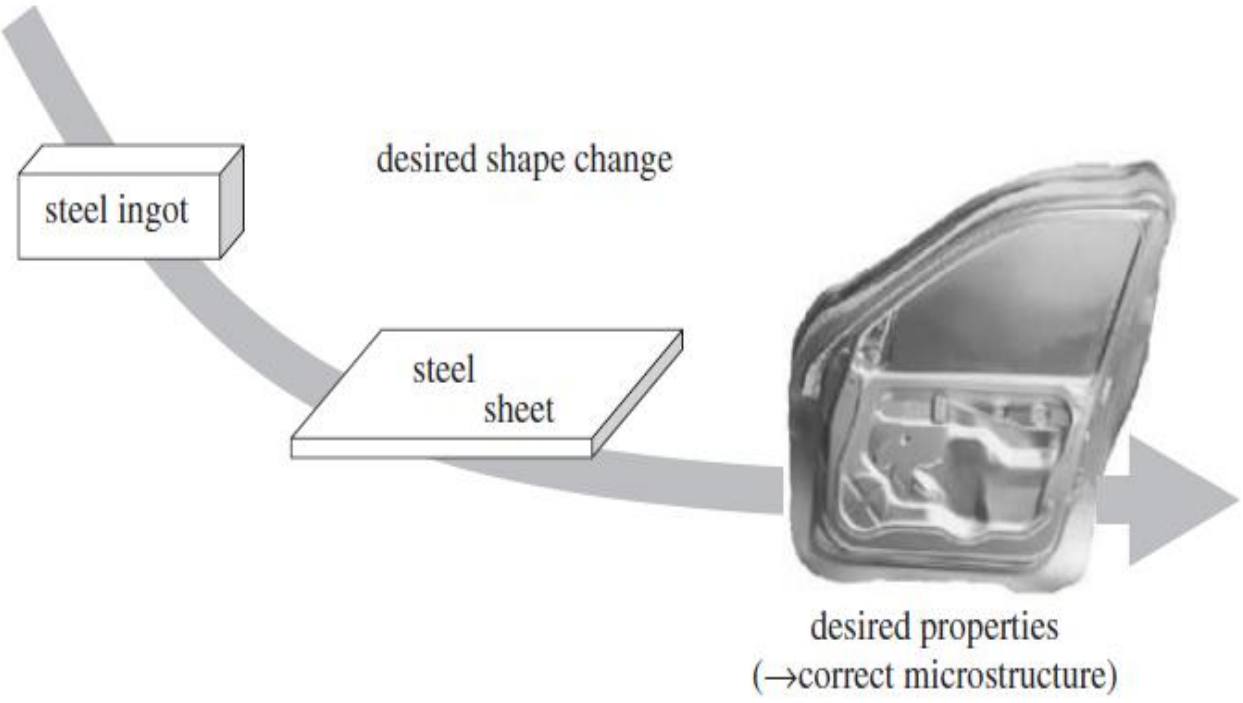

Figure (1.2): Steps of Thermo Mechanical Processing.[5]

The controlled softening of micro alloyed steel during thermo-mechanical processing make the product suitable to accomplish the fancied properties of high strength, toughness, ductility and good weld ability in API micro alloyed line-pipe steel [6].To acquire high review of API steel is to controlled thermo-mechanical processing and cooling rate has been a matter of sympathy toward an extensive number of steel maker. Therefore, the mechanical properties of API high strength steel might be amazingly enhanced through fitting determination of suitable composite arrangement and proper selection of TMP parameter that refine and homogenise the final microstructure. In the seventies, the hot rolling and normalizing was supplanted by thermo-mechanical rolling. The latter process empowers materials up to X 70 to

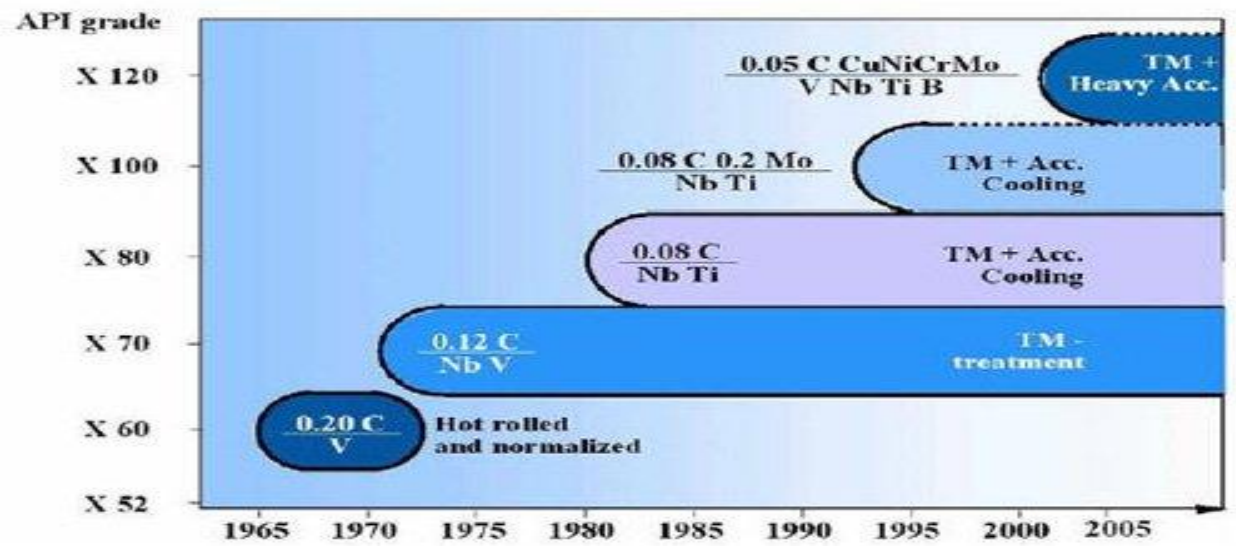

Fig(1.3): The enhancing role of Thermo-mechanical process year by year[7].

Be produced from steel that are micro alloyed with Nb and vanadium and have lessened carbon content. An enhanced preparing strategy, consisting of thermo mechanical rolling moving in addition to ensuring quicker cooling process which has developed in eighties. By this system, it has become possible to produced higher strength material like X 80, having a further lessened carbon content and accordingly great field weld capability.

To summarize, **main objective** of this study are as:

i. To obtaining a microstructure of Acicular/Ferrite in API-X60 grade pipeline steel by using Thermo-mechanical processing.

ii. To apply the standardize procedure for unambiguous analysis of microstructure by using EBSD/OIM and SEM analysis.

CHAPTER NO: 2

LITERATURE REVIEW

2.1 PIPELINE GRADES

Natural gas is an undeniable alluring vitality source, however major reserve are often remotely located from potential markets. High operating pressure and /or thin wall pipes are intends to lessen a gas transmission costs, however traditional steels are ordinary needed sufficient quality. In the course of recent years, the trends towards expanded transportation effectiveness have to a great extent accomplished by expanding the width of pipelines. Historically the pipelines business has been higher evaluations at the rate about 69MPa(10ksi)/decade(Tamehiro&Chino,1991)which are shown in fig(2.1)[8].The highest grade pipeline in commercial development today is X-100,consistent with historical trends. The properties of the pipe line steel needs to be equivalent with the measure of the standards of the American Petroleum Institute (API). The API steels are of different grades depending on the composition, properties and thickness. The numbers in these designations refer to the minimum yield strength (ksi) of the finished pipe [9]. The properties in API steels are essentially obtained by addition of various micro alloying components [10, 11] for example Ti, B, P, N, S, Mn, V, Nb etc. and so forth the controlled TMP and cooling. The properties of the pipeline steels may be characterized as blend of strength, fracture toughness and weld ability, which is accomplished through thermo-mechanical, controlled processing (TMCP).

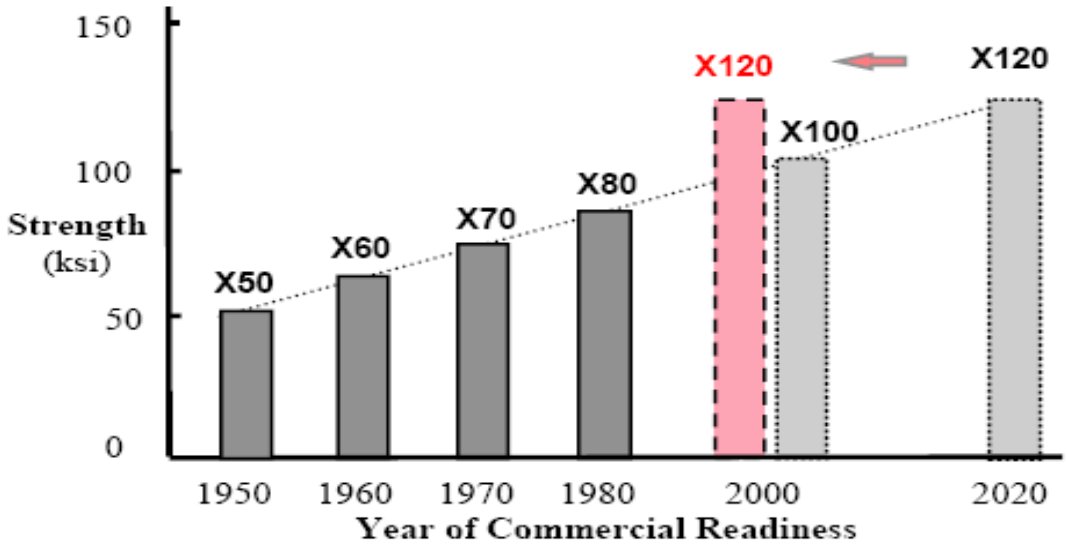

Figure (2.1): Commercialization of pipeline technology (ksi/0.145=MPa)[8]

The typical composition range of various API grade steel such as X60, X70, X80 etc. is shown in Table 2.1[12-14]. This entails selection of a suitable alloy composition which conforms to various standards of the API and the correct selection of the TMCP parameters to achieve the desired micro structural contents that leads to required properties. The recommended yield strength and tensile strength of API steel are as per ISO 3183:2007 (modified) for petroleum and natural gas industries [9].

Table 2.1

Chemical composition (in wt %) range of API X60, X70 and X80 grade steel [12-14].

API	Elements (wt. %)													
	C	**Si**	**Mn**	**S**	**P**	**Al**	**Ti**	**V**	**Cu**	**Ni**	**Cr**	**N**	**Mo**	**Nb**
X60	**0.7**	**0.2**	**1.5**	**0.01**	**0.014**	**0.035**	**0.01**	**0.04**	**0.17**	**0.09**	**0.01**	**-**	**0.01**	**0.03**
X70	**0.06**	**0.18**	**1.55**	**-**	**-**	**-**	**0.017**	**-**	**-**	**-**	**0.02**	**0.0071**	**-**	**0.055**
X80	**0.056**	**0.31**	**1.90**	**0.0015**	**0.011**	**0.029**	**0.018**	**-**	**0.044**	**0.221**	**-**	**0.0044**	**0.213**	**0.046**

Maximum and minimum limits of recommended yield strength and tensile strength of these various grades of pipe line steel is tabulated in Table 2.2 [11]. API grade steels are generally obtained in the form of as rolled, normalizing rolled, thermo-mechanical rolled, normalized and tempered or quenched and tempered plates etc. The thermo-mechanical process is a common term described as the plastic deformation of steel during heat treatment to improve the mechanical properties by appropriate design of hot rolling and subsequent cooling process path**.**

Table 2.2

Yield strength and Tensile strength of API grade steel pipes standard [9]

Pipe grade	Pipe body of seamless and welded pipes			
	Yield strength (MPa)		Tensile strength (MPa)	
	Minimum	Maximum	Minimum	Maximum
X52	360	530	460	760
X56	390	545	490	760
X60	415	565	520	760
X65	450	600	535	760
X70	485	635	570	760
X80	555	705	625	825

2.2 Role of Alloying Elements

The API grade steels have a variety of chemical compositions based on the requirement properties, these steels are characterized on the basis of their leading micro-alloying constituents. The effects of major alloying elements in the properties of API grade steel are given below in table 2.3[15-26].

Table 2.3

Major effects of alloying elements in High Strength Line Pipe Steels [15-26]

Element	Effects
C	•Matrix strengthening (by precipitation). •Formation of ferrite, bainite and martensite largely depend on C%. •Improves hydrogen induced cracking [HIC] resistance •Excess C in alloy decrease toughness, weld ability and ductility.
Si	•Improvement in strength (solid solution), Matrix strengtheners. •detrimental effect on both base steel and HAZ toughness, improves ferrite ductility by increasing driving force for carbon migration in austenite, suppresses carbide formation
Mn	•Matrix strengtheners. •Delays austenite transformation during cooling •increases harden ability •Decreases ductile to brittle transition temperature •Indispensable to obtain a fine-grained lower bainite microstructure
S	•Reduces low temperature toughness, hot shortness •Forms elongated MnS after rolling thus forms starting points for HIC
P	•Detrimental effect on pipe making and field weldability. •Segregate at centre in casting steel slab and cause grain boundary fracture
Al	•Fixes free nitrogen in HAZ • decreases toughness and formability • Fine oxide dispersant during deoxidation.
Ti	•Grain refinement by suppressing the coarsening of austenite grains (TiN formation) •Strong ferrite strengtheners. •Fixes the free Ni (prevent detrimental effect of Ni on harden ability)
V	•Leads to precipitation strengthening during the tempering treatment •strong affinity to carbon and nitrogen •With Nb, reduces HAZ softening •VN precipitate predominant ferrite strengtheners.
Cu	•Improves corrosion resistance (with Cr and Ni) and HIC • restricts hydrogen formation by forming a protective layer •lowers austenite to ferrite transformation temperature •high copper content can cause embrittlement crack at time of hot rolling •higher amount of copper induces excessive precipitation hardening

Ni	•Improves the properties of low-carbon steels without impairing field weld ability and low temperature toughness • In contrast to Mg and Mo, Ni tends to form less hardened micro structural constituents detrimental to low temperature toughness in the plate (increases fracture toughness) •increases bainitic fraction
Cr	•Improves strength and quench hardenability • improves corrosion and HIC resistance • lowers carbon activity in ferrite, high strength, low YS/UTS
N	•TiN restricts austenite grain growth and improves low temperature toughness
B	•Improves quench hardenability with Nb and Mo, helps forming lower bainite and lath martensite
Mo	• Suppresses austenite recrystallisation and grain growth •Improves hardenability and strength, thereby promotes the formation of the desired lower bainite microstructure
Nb	•Reduces temperature range in which recrystallization is possible between rolling passes •Retard recrystallization and inhibit austenite grain growth (improves strength and toughness by grain refinement) •NbC effective strengtheners than VN •higher solubility in austenite at low carbon level •Promotes refined ferrite and large volume fraction of acicular ferrite

2.3 Role of Micro structural constituents in Pipeline Steel

The main focus on application of micro alloyed steel is to improve the efficiency of transportation at higher pressure and transmission rate over long distances at extremely low temperatures. Therefore, the pipe line steel must have high strength and high toughness at extremely low temperature. These properties are usually obtained in API grade micro alloyed steel with ultra-fine ferrite grain sizes having some fraction of bainite and Martensite-Austenite constituent well known as MA structure. Figure 2.2 shows the micro structural evolution of line pipe steel grades in terms of microstructure leading to improved strength and toughness over the last few decades as well as a short description of the main alloying elements and processing applied [29-31] and fig(2.3)optical micrographs which support the figure 2.3. [32]. To be able to practice controlled rolling and thereby achieving the desired final mechanical properties of the product, knowledge of the micro structural evolution is essential. The micro structural constituents in the final plate after cooling are indicated by the grain size, fraction of various constituents e.g. polygonal ferrite, pearlite, acicular ferrite, bainitic ferrite, bainite, martensite, etc.[64-65]. The volume fraction and size of precipitates and dislocation density of atom at the grain boundary improve the final strength of material . The solid solution strengthening does not vary much with the composition range; and the size and volume fraction of precipitates also has reasonable effect on strength [66]. Therefore, the most important factor to control during the process is the grain size.

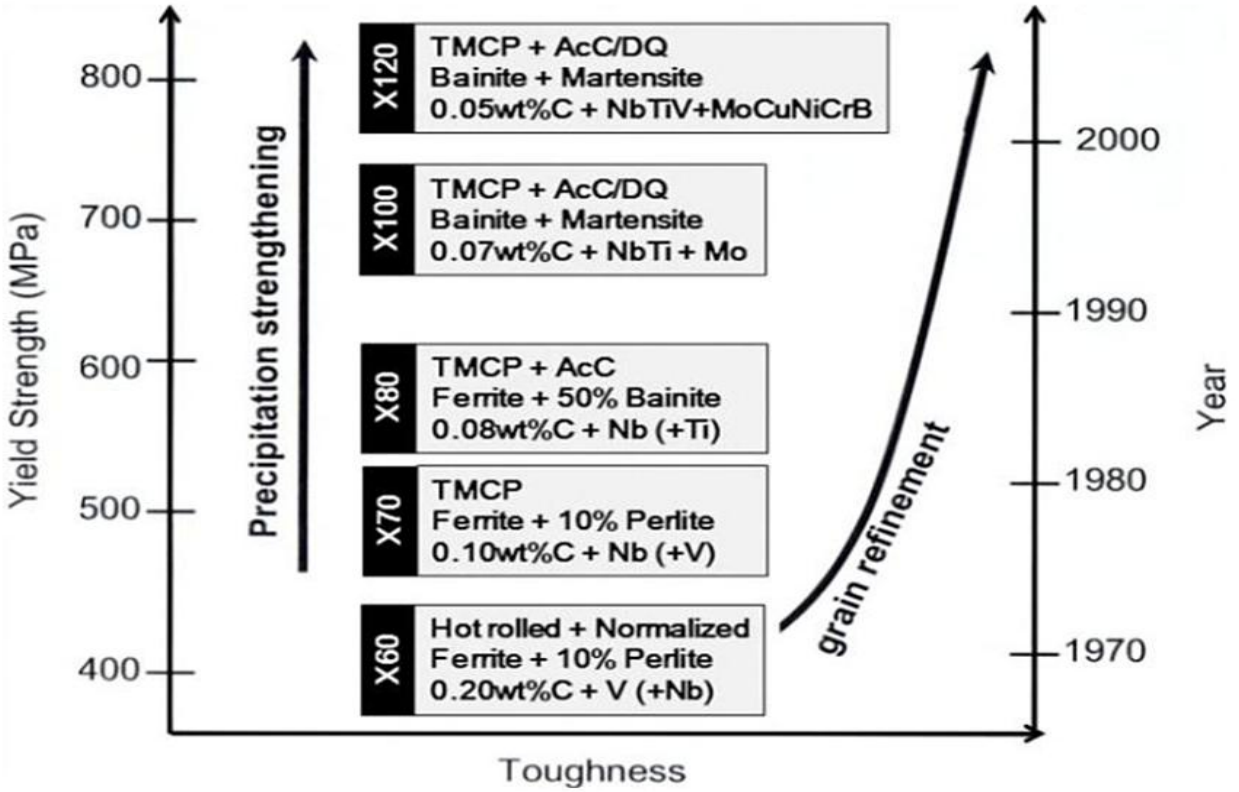

Fig. 2.2: Evolution of line pipe steel grades as an example of HSLA steel development [29-31].

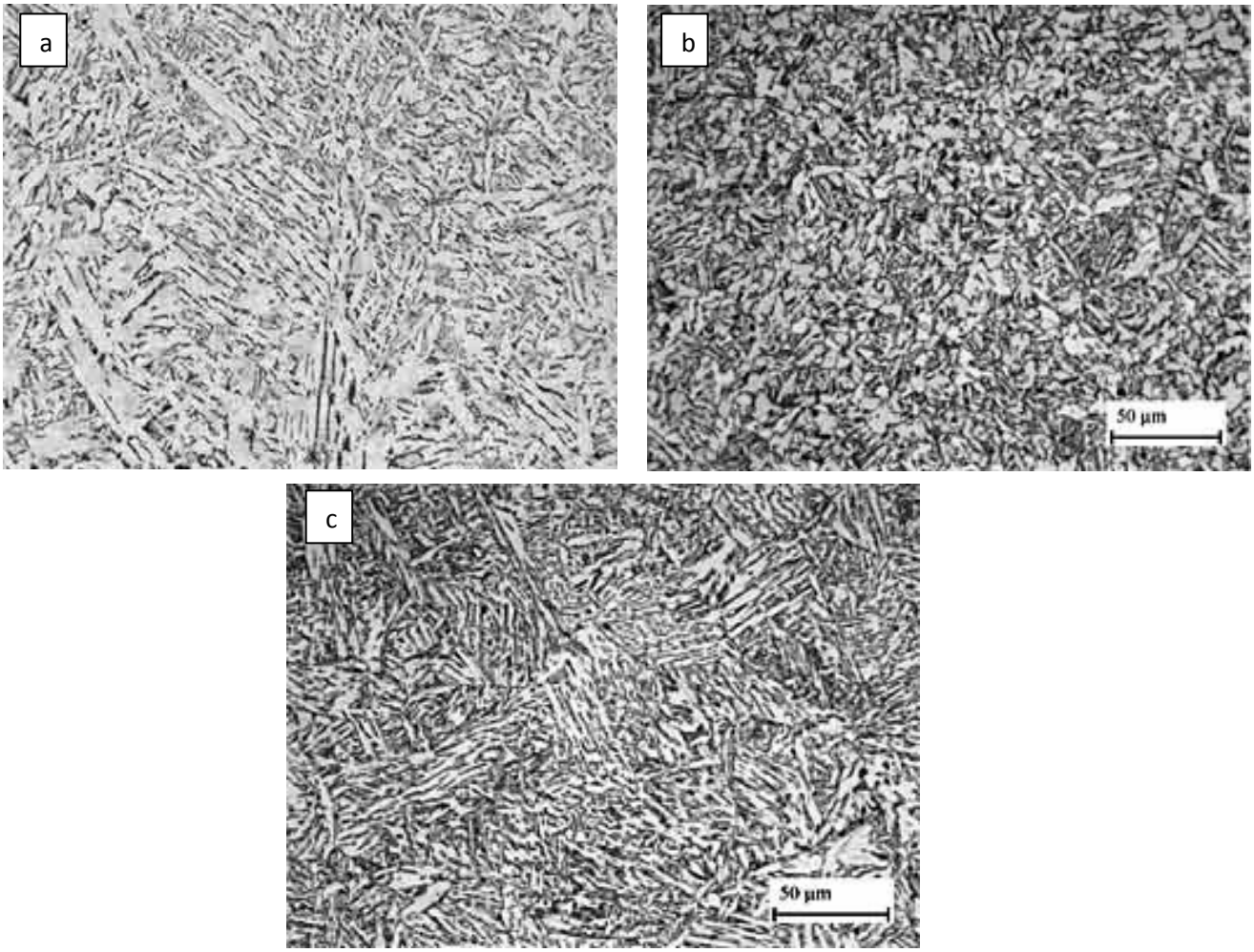

Figure 2.3Optical image of (a) Ferrite+pealite (b)Ferrite+Bainite (c) Bainite+Martensite [32]

The alloy addition such as Nb,Mo,V can help to formation of acicular ferrite by making the favourable environment for retarding the recrystallisation and also suppress the formation of polygonal ferrite and ferrite transformations [67]. Increases in the Cr+Mo+Ni+Cu from 20 to 10 ^{0}C/s and for the formation of acicular ferrite from 10 to 5 ^{0}C/s [67-68]. To achieve the desired microstructure features such as increased harden ability, more alloying elements such as Nb,Mo,Cr& V becomes a necessity, but in controlled manner, to avoid maretnsite formation in the heat affected zone of the welded plates. The additions of Mo reduces diffusivity of carbon that leads to carbon enriched austenite and promotes M-A formation and also ,this additions delays the precipitation of carbides (NbC) that eventually adds to grain refinement. At higher operating depth, low temperature toughness is required and which is totally depend upon the fraction of martensite to austenite constituent, as increase in their ratio leads to increase tensile strength. If increasing bainite fraction, then martensite to austenite constituent gives rise to lower value of low temperature toughness. This can further improved by increasing the high angle grain boundaries that help in increase the low temperature toughness and decrease in the ductile to brittle transition.

2.3 .1 Role of Acicular Ferrite/Bainite Microstructure in Pipe Line Steel

It is a microstructure of ferrite in steel and it is characterised by needle shaped microstructure (in view of 2D) and it is advantages over other microstructure because it has chaotic ordering (Lack of order) which increase the toughness because acicular ferrite nucleate in a non-homogenous manner on a small non-metallic inclusion along it boundary and expand in many different direction from the point of nucleation sited of non-metallic inclusion. By this above characteristics the cleavage crack does not cross the grain boundary of acicular ferrite because its having the property of high of high angle grain boundary which radiate the cleavage crack in another direction. By this way it gives the superior characteristics of material which is known as toughness. [33]

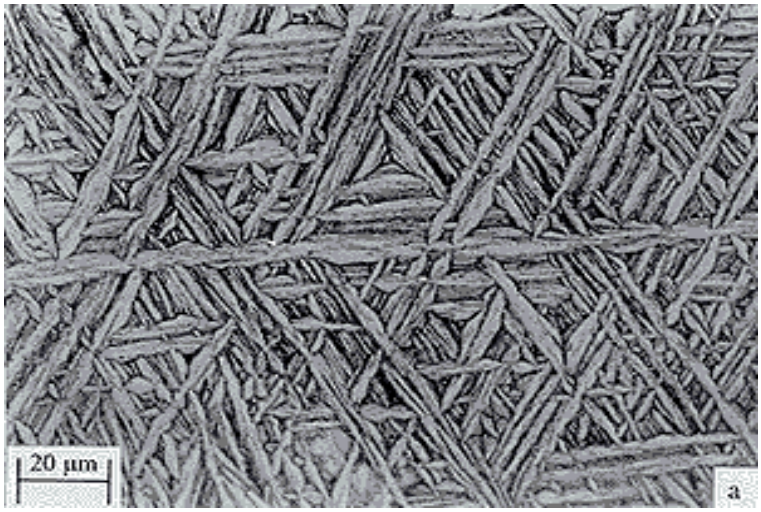

Figure 2.4. Optical Image of Acicular Ferrite having needle like shape. [32]

It occurs at below Bainite start temperature .The combination of different alloying element in material also plays a very important role for creating the favourable environment for the formation of acicular ferrite in which Nb &V play vital role because Nb in steel can effectively reduces the recrystallisation temperature and rise the non-recrystallisation temperature (T_{nr}) by giving his presence by either in the form of solute drag effect in the solution or in the form of precipitate .Under which strength of material will increased by promoting the formation of fine ferrite microstructure.[33] Due to good combination of toughness and strength acicular ferrite is a desirable microstructure in pipe line steel because it meets the level of requirement at cheap cost.

2.4 Role of Thermo-mechanical Processing

The basic role of thermo-mechanical processing is to improve the final microstructure of the specimens which having good combination of mechanical properties such as toughness, weldability and strength. It describes the set of reheating and hot rolling operation by which relatively simple, basic materials are converted into high quality components under given combination of micro-alloying additions. The most important is grain size of ferrite which is basically depend upon the prior austenite grain size, deformation temperature conditions and austenite grain and the deformation substructures and precipitates which may nucleate ferrite and including the nature of the austenite to ferrite transformation, whether diffusion or displacive.During the thermo-mechanical processing ,the specimen which are heated to a austinization temperature and then soaked at these temperature for certain interval of time. After soaking for certain period of time, it strained through multipass schedule under following the continuous cooling conditions and then cooled to room temperature. Figure 2.3 is a line diagram representation of the thermo-mechanical processing for API-X60 grade steel [34] indicating the critical temperatures (soaking temperature (T_s), non-recrystallisation temperature (T_{nr}), phase transformation temperature (A_{r3}, A_{r1}).

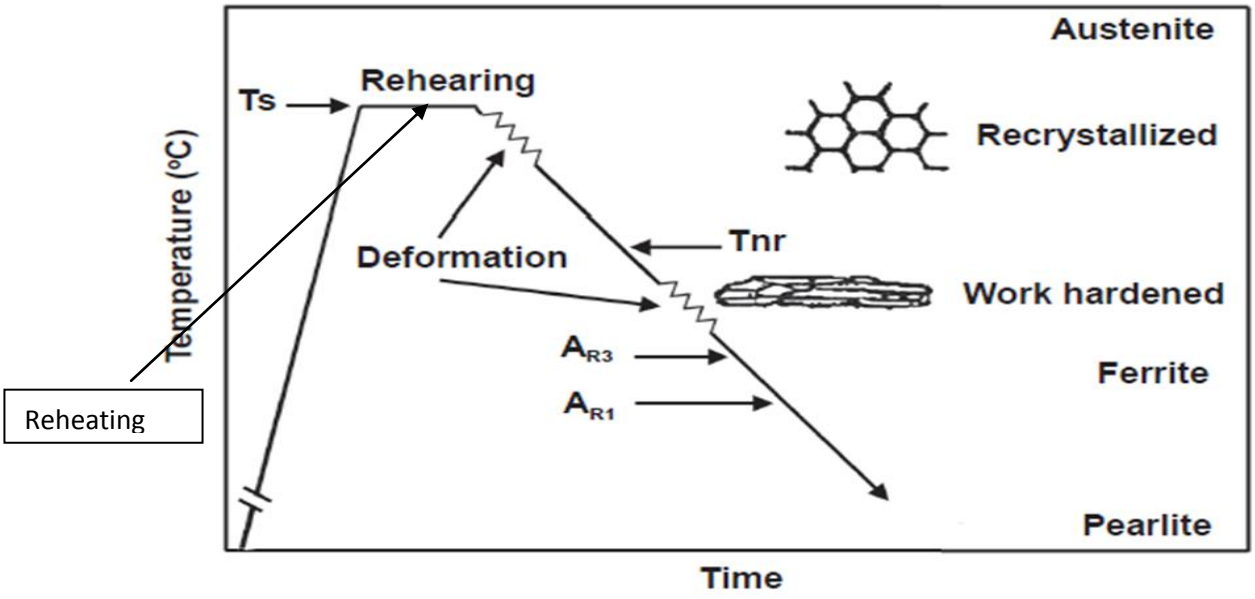

Figure (2.5) Line diagram representation of the thermo-mechanical processing for micro alloyed steel, indicating the critical temperatures [34].

The material for the most part quits recrystallising underneath a certain temperature throughout hot rolling during hot rolling. This temperature is often called the recrystallisation stop temperature (RST) or the non-recrystallisation temperature (T_{nr}). The T_{nr} denotes the temperature above which static recrystallisation occurs between passes [35-37]. It depends upon the deformation temperatures, the cooling rate and underpass time in the rolling process.

2.4.1 Recrystallisation mechanisms

Recrystallisation mechanism is an critical device to getting desired microstructure and mechanical properties in an austenite phase .As steel deformed under distinctive temperature then internal energy is increase as accumulation of dislocation and simultaneously various softening process occur which diminish the internal energy.

It is the shaping of new strain free equaxied grain structure by movement of high angle grain boundary on the expense of stored energy in thermo-deformed materials. The recrystallisation methodology to huge degree relies on the temperature, time, strain and strain rate, until the recrystallisation is finished. It is the mixture of grain nucleation and development process. Throughout this period, continuous deformation reasons dislocation gathering. In the event that the dislocation density build over the basic worth needed for DRX which is subject to the deformed conditions. New, progressively recrystallised grain cores will be shaped on the lengthened limits of the first grains and start to develop.

2.4.2 Dynamic Recrystallisation (DRX)

It is defined as the formation of new-strain free equaxied grains under the application of thermo-mechanical treatment and it is one of the main softening mechanism which is carried out after attaining the critical value of strain .Schematic description of the flow behaviour of steels at high temperature is shown in Fig. 2.4 [38].The flow curve associated with dynamic recrystallisation can be of two forms i.e., cyclic, indicates grain coarsening, and single peak indicates grain refinement. When the softening process is proceed by dynamic recrystallisation then flow curves has attained to steady state regime after passing the peak point which are shown in (fig2.4).Basically, the flow curves has divided into three stage in which first stage has occurred due to occurrence of work hardening and dynamic recovery which relatively occur at low strain.

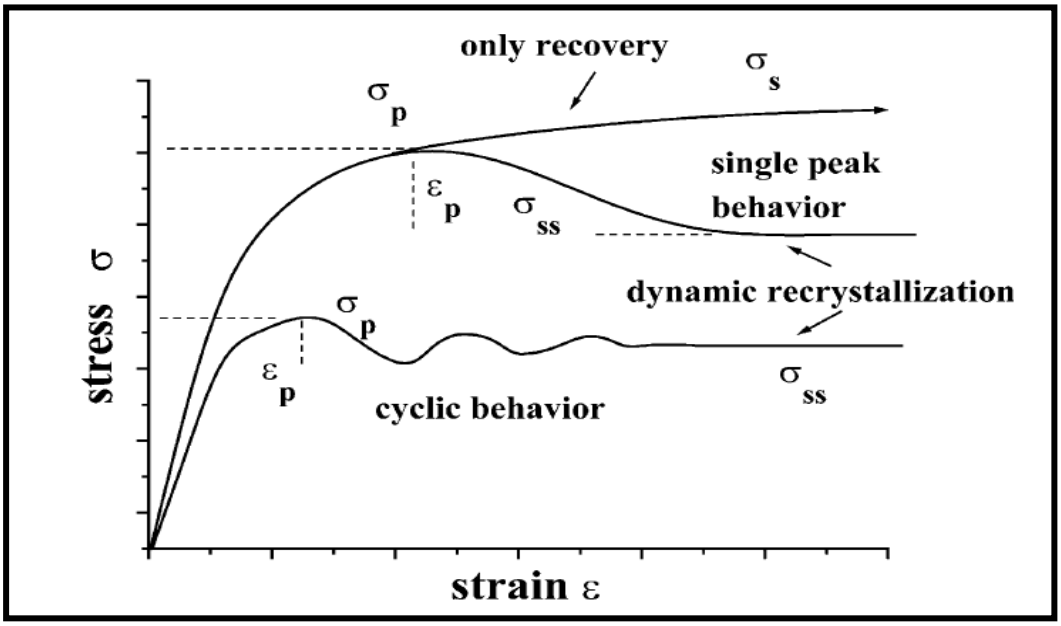

Figure 2.6. Line diagram representation of the flow behaviour of steels at high temperature.[38]

At this stage there is multiplication of dislocation density and more elongated grain which deformed in one particular direction which is called "pancake" microstructure and there another phenomenon has occurred in which formation of sub grains in deformed large grains. At large strain, there is steady state regime has occurred with the formation of strain free equaxied grain structure. The two stage which has discussed earlier are separated by another zone which is called transition zone in which the true stress value has dropped from pervious value by showing certain changes in the curve which are as: [38]

1.By formation of single peak at low temperature and low strain rates.

2.By formation of multiple peaks at high temperature and low strain rates.

2.4.3 Role of T_{nr} (Non-Recrystallisation Temperature)

The role of T_{nr} is very important in upgrading the strength of the material because it basically indicates the state or conditions of material at which there no formation of new strain free, equaxied grains in the material but only deformed grained has developed in particular fashion. When material deformed below T_{nr} then it leads to work hardening and therefore formation of "pancaked" grains boundary area which increase the number of nucleation sites for the austenite-to ferrite transition and ma45y promotes fine grained microstructure producing a plate with good balance of strength and toughness [39]. From the given below figure(2.5) it can easily shown that how % fine ferrite is going to increase and here the term T_r is introduced which known as recrystallisation stop temperature which is far below than T_{nr}.

If the deformation occur above the T_{nr} results in equaxied recrystallisation grains and grains become large due to grain coarsing.

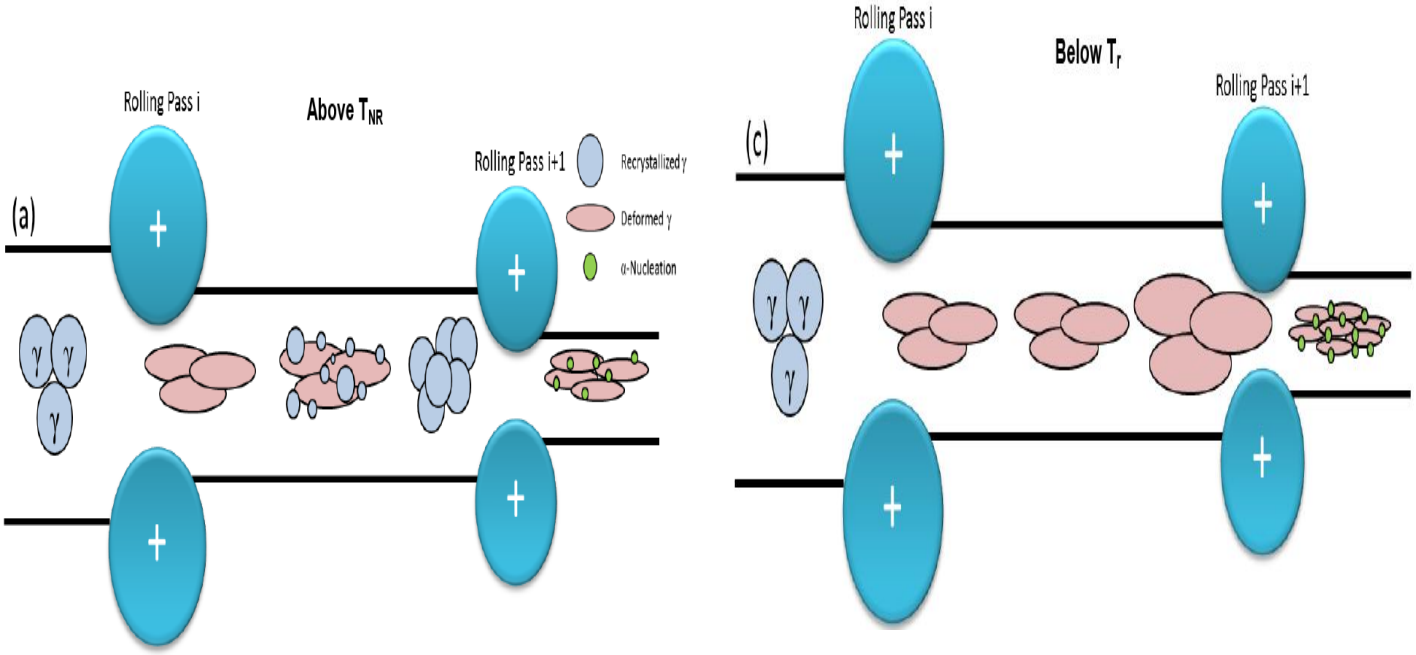

Figure: 2.7: Schematic view which represent the deformation above and below T_{nr} [40-41].

It can be calculated by various method which are as:(1) Empirical Method (2) Laboratory Method.Here,I discuss only empirical formula to calculate T_{nr} because it is a easy and useful to calculate in which are as

Boratto Equation:

$$T_{nr} = 887+464C+(6445\ Nb - 644\sqrt{Nb}) +(732V-230\sqrt{V}) + 890\ Ti+ 363\ Al - 357\ Si.[42]$$

Bai Equation:

$$T_{nr} = 174 \log\left[Nb(C + \frac{12}{14} N)\right] + 1444.[43]$$

Flecture Equation:

$$T_{nr} = 203-310C - 149\sqrt{V} + 657\sqrt{Nb} + 683\ e^{-0.36\varepsilon}\ [44]$$

From, here I am discuss on the synergistic effect of V,Nb and Ti on the T_{nr}.Each of the micro alloying are transition metals and form solid solution with iron [45].Vandium,Nb and Ti are all known for grain refinement strengthening through grain boundary pinning and precipitation strengthen through the formation of carbides ,nitrides or combination of called carbon nitrides (C,N) and this happens when it retard the recrystallisation and increase the non- recrystallisation temperature (T_{nr}) in this way that it forms the

favourable environment for the formation of acicular ferrite/bainite microstructure.As,we known that it is good combination of strength and toughness.

From, the given below figure we can understand that how the role of micro alloying element affect the non-recrystallisation temperature.

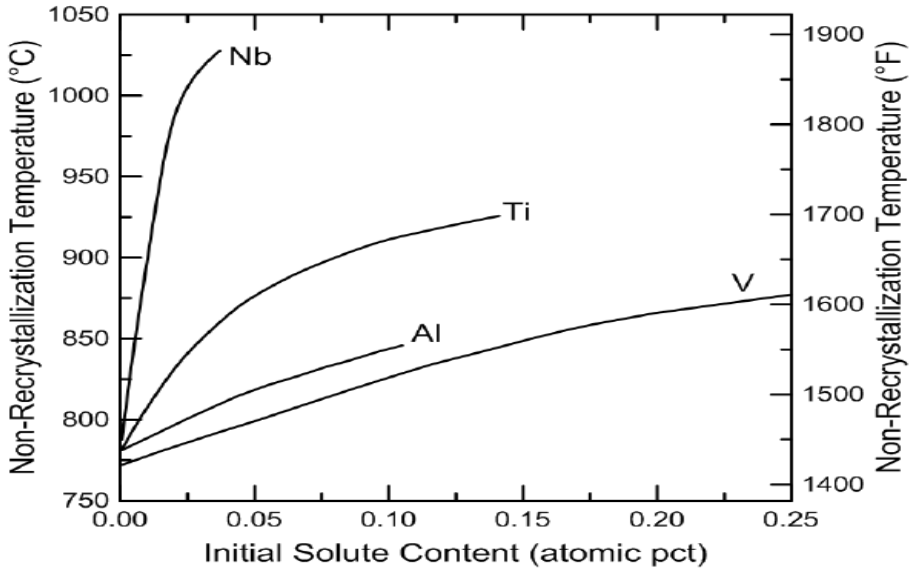

Figure (2.8): The effect of alloying element on non-recrystallisation temperature.[46]

2.4.4 Fractional Softening

It is defined as that the volume fraction of recrystallised volume of grain which mainly occurs at high temperature under expense of stored energy of specimens. It easily takes any shape under the application of small amount of external force and it mainly characterised by S-shaped curve which basically indicated that transformation rates. During initial stages transformation rate is slow and fast at end stages. In between two stages the transformation rate is fast because nuclei grow into particles and consume old phase. [47]

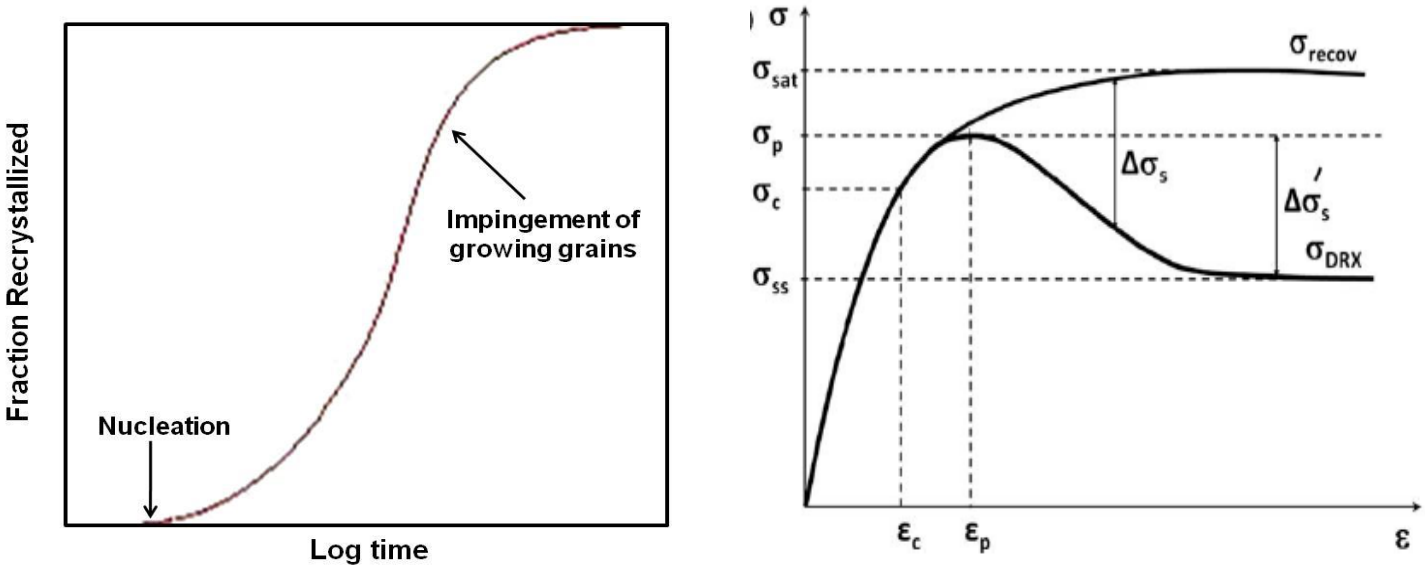

Figure 2.9.(a)Typical recrystallisation kinetics [47],(b)Schematic diagram which illustrate the work hardening curve associated with typical experimental DRX flow curve [48].

Fractional softening is controlled by 2 parameters which are as (1) Critical strain (ε_c) which is required for the initiation of DRX.(2) The strain at which rate of softening is maximum. The method by using this, we can calculated the fractional of recrystallised volume in the first one is the calculation the difference between the curves of $\sigma_{recovery}$ (dynamic recovery) and σ_{DRX} (dynamic recrystallisation stress).The difference between the curves is directly indicated as $\Delta\sigma_s$ which is known as net softening which directly attributable is DRX.Finally the fractional softening has calculated by using the formula which is expressed by $X= (\sigma_p-\sigma_{ss})/ (\sigma_{sat}- \sigma_{ss})$.[48].

2.5 Thermomechanical processing methods

2.5.1. Rolling

Rolling is a process of plastically deforming metal by passing it between rolls and it is the most widely used forming process in which high productions and close control of final product is possible. Hot rolling, as with all hot working process requires elevated temperature control, generally in the range 850°C-1320°C for steel[50]. The lower flow stress of the material at high temperature leading to lower tool forces and power to deform the plate [51]. The work piece is heated to a uniform elevated temperature in the austenite region, typically above the T_{nr}. The T_{nr} for the steel is alloy dependent and also dependent on the deformations parameter [40-43]. For micro-alloy steels, the reaustenitizing temperature, or soak temperature is often between 1200^{0}C & 1320^{0}C.The steel is then cooled & rolled at a given deformation temperature. Hot rolling of steel previously began with a primary roughing mill (also called blooming, slabbing or cogging mill)[52].A roughing mill is usually a two- high reversing mill with 0.610-1.37 m diameter rolls. An ingot is broken down into blooms or slabs for further processing of plates, bars or sheets. The initial breakdown passes usually only involve small reductions. Significant spreading of the ingot width occurs during hot rolling. Ingots are rotated 90^0 during intermediate passes and often pass through edging rolls or grooves to maintain desired dimensions [53]. An ingot may go through one reversing mill (10-20) times before moving to subsequent process with industrial improvements continuous casting of slabs is now used in high productions plants where slabs are produced directly from the molten metal.

Plates are produced from reheated slabs or ingots.Fig.2.4 shows the flow of rolled materials in various mills. [54] .Utilizing slabs to roll plate steel, instead of ingots, allow achievements of better surface quality and yield improved mechanical properties, improved temperature control and greater output due to fewer passes. Dedicated plate mills are capable of rolling product (2.54-5.08) m wide. A slab is sent to a reheat furnace to be heated to a desired temperature. The slab then goes through the roughing mill, which consist of a series of vertical a horizational mill stands. A shear is used typically to remove the head and tail before entering the finishing mills. The finishing mill utilize one or a series of horizontal mill stands and loppers to maintain desired strips tensions by pushing a free rotating roller against the strip.[53-54].

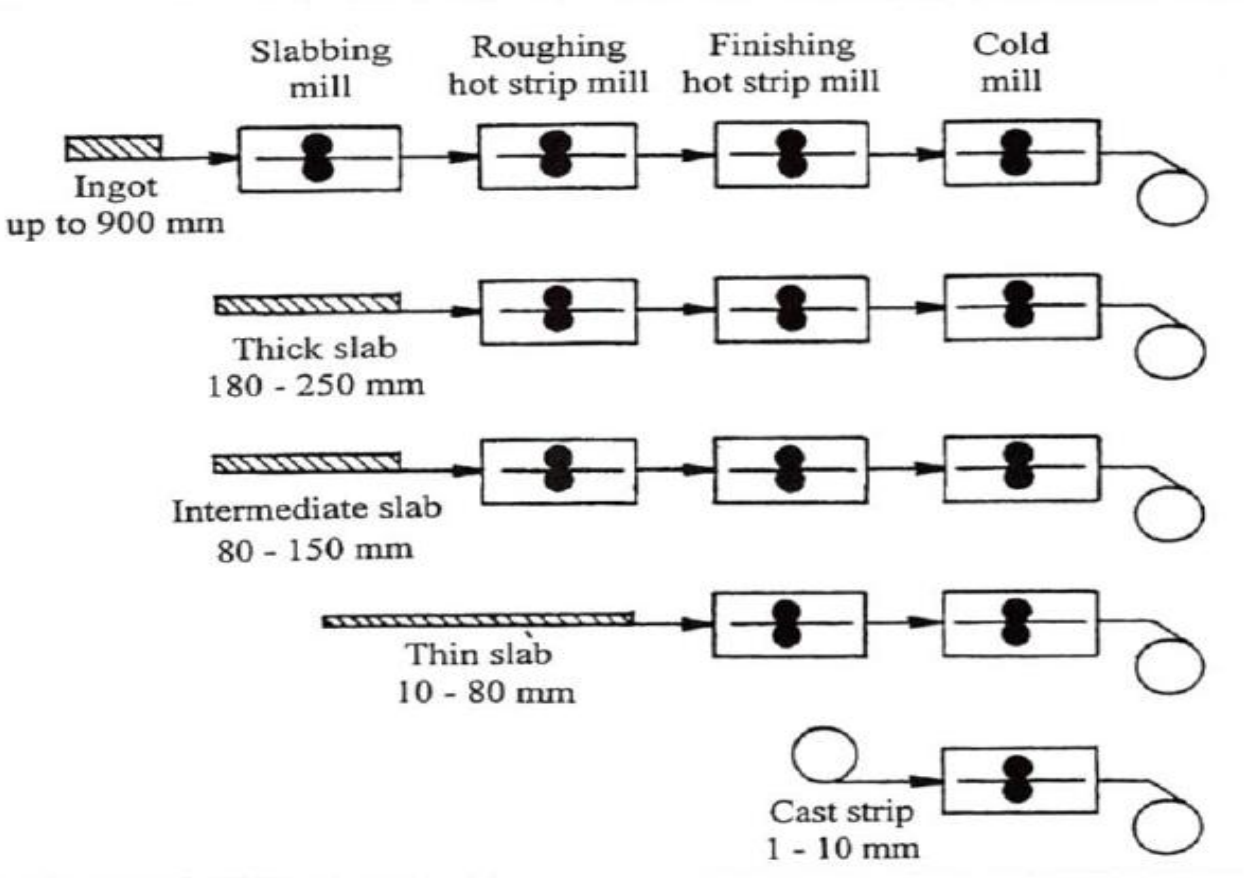

Figure (2.10) Flow of rolled material through various mills. [55]

Depending on the desired properties, hot rolling can be terminated approximately 50^0C to 100^0C above the T_{nr} to ensure uniform fine grains and prevent the possibility of strain –hardening. Deformations below T_{nr} leads to work hardening and therefore the formations of "pancake" grain boundary area increase the number of nucleation sites for the austenite- to ferrite transitions and may promote a fine grained microstructure producing a plate with good balance of strength and toughness properties.[52-53].

2.5.2. Deformation Dilatometer

It is basically used for heat treatment of metal and alloy and controlling it isothermal dwell time, heating rate, and cooling rate and these are the factors which play a very important role for controlling the physical characteristics of the material. It works on micro scale level that can easily observe the small changes in dimension. By using this, we can easily generate the TTT diagram and CCT diagram, which are important tool for any kind of analysis. The DIL805 series type deformation dilatometer which cover widest range of deformation conditions and also used for accurate characterization and processing of materials.[56]

2.5 .2.1. 805L Quenching Dilatometer

It is self controlled automated type quenching dilatometer which is basically used for examine the dimensional changes under extreme case of heating and cooling. Figure 2.5 is a schematic representation of DIL 805L deformation dilatometer. In which solid or hollow sample is inductively heating up to a high temperature level of 20^0C to 1500^0C and for the range of cooling is about -150^0C to 1300^0C.When transformation occur either in case of heating and cooling then it indicates the micro change in dimensional of specimen.[57]

Figure (2.11) Top View of DIL 805L Quenching dilatometer.[57]

2.5 .2.2. 805A Quenching Dilatometer

It is new benchmark technology for calculating the dimensional change in a specimen at micro-level under different phase of transformation of steel alloy which carried out at various level of heating and cooling. The main characteristics of the deformation dilatometer is working in the range of -160^0C to 1500^0C with heating rate is 400k/s and with cooling rate is 2500k/s. Its versatile characteristics of its design such as it easy to accommodate many different modules including the 805D deformation adapter and other measuring head such as DTA/DSC.By this way, these characteristics make powerful instrument for calculating the critical parameter of steel manufacturing and heat instruments. [55]

.

Figure (2.12) Top View of DIL 805A Quenching dilatometer.[57]

2.5 .2.3. 805D Deformation Dilatometer

It is that type deformation dilatometer which basically used for getting the details regarding to time temperature transformation which occurred in materials after deformations. The basic principle of this deformation dilatometer is that in which sample are composed by using various deformation programs such as linear, multilevel under the application of constant deformation of force with constant rate. Figure 2.7 is a schematic representation of DIL 805D deformation dilatometer. There no limit for providing the number of deformation steps with a pause between steps of only 40ms and this unique property makes it able to control the cooling rate and deformation process a way that it creates DTT diagram. [58]

Figure 2.13: Top View of DIL 805A Deformation dilatometer.[58]

2.5.3. GLEEBLE

It is fully integrated closed loop control thermal and mechanical system which provides the friendly environment for any kind of data analysis which base on number of mechanical test and physical simulation programs. The heating system which inbuilt in it is capable to heat the specimens up to the rate of 1000^0C/sec or can hold steady state programs and its high thermal conductivity makes the system cool at a very high cooling rate .The thermocouple or an infrared pyrometer can grip the feedback control system for getting accurate reading under high speed of heating because it works up to 3 to 10 times faster than conventional working machines. It is fully integrated servo hydraulic servo system which are capable for applying the static load about 20 tonnes in compression and 10 tonnes in tension and displacement rate in which can achieved by gleebel is about 200mm/sec.It is fitted with LVDT transducer load cell which play very important role for providing accurate and precise measurements in control way under any given tests. These versatility characteristics of gleeble make capable for simulate many thermal-mechanical process. By

this way operator can control any variable regarding to any test at any time. The main heart of gleeble machine is series 3 digital control systems which play a very important role for controlling the all necessary variables regarding to thermal mechanical tests. By this way it can control by annual way, automatic or combination of manual automatic which needed to provide maximum versatility in material testing.[59]

Figure 2.14. A view of Gleebel System.[59]

It consist of window based workstation and embedded with powerful controlled system which offers multitasking property to gleeble .By this way it make suitable machine for industry in which multiwork can controlled in simultaneous manner. The gleeble machine is fitted with different software tool which make easy for operator that create any test on workstation through number of programming options including QuickSim software. The QuickSim Software which embedded in gleeble play a very important role or providing wave of arbitrary programming which work under differ thermal and mechanical systems. Under different characteristics it can easy to operate by manually or automatically at any time and once the test has completed then it automatically uploaded the data into origin software. [59]

CHAPTER NO: 03

EXPERIMENTAL APPROACH

3.1 Materials used

The starting material for our investigation is API-X60 grade micro alloyed steel supplied by M/s Tata Steel Jamshedpur and available in the form of rolled plate ~ 7mm thickness. The chemical composition of the sample is analysed using a optical emission spectrometer and the chemical constituents are given in Table 3.1. Samples of 5 mm diameter were machined out of these plates for conducting deformation studies.

Table 3.1

Chemical compositions (wt. %) of API-X60 steel with remainder being Fe

C	Si	Mn	S	P	Al	Ti	V	Cu	Ni	Cr	N	Mo	Nb
0.08	0.19	1.43	0.04	0.012	0.031	0.02	0.01	0.033	0.037	0.125	0.004	0.009	0.03

3.2 Thermo-mechanical Process Schedule

The Thermo mechanical processing of API-X60 micro alloyed steel was achieved in the form of high temperature compression experiments performed in a deformation dilatometer facility available at RWTH Aachen University, Germany. The deformation experiments were conducted with focus on evolution of recrystallisation kinetics and microstructure which based as a function of rolling temperature, strain with constant strain rate after hot deformation. Figure 3.1 shows the main features of TMP schedule which is conducted at deformation temperature of 900^0C, 10000C and 1100^0C respectively.

The hot compression test specimens were solid cylinders with a diameter of 5 mm and a length of 10 mm. The specimens were heated to 1200ºC with a heating rate of 3ºC/s. After holding at this temperature for 20 min, specimens were cooled to the deformation temperatures of 900, 1000 and 1100ºC at a cooling rate of ~10ºC/s. The samples were deformed with different value of strain such as 0.4, 0.8 and 1.2 with fixed strain rate which is 2 s^{-1}. After hot deformation, specimens were quickly quenched by water to retain the state of hot deformed austenite. Experimental parameter for deformation studies is representing in Table 3.2. The true stress and true strain curve of the deformation tests were plotted to obtain the flow curve and understand the nature of recrystallization kinetics.

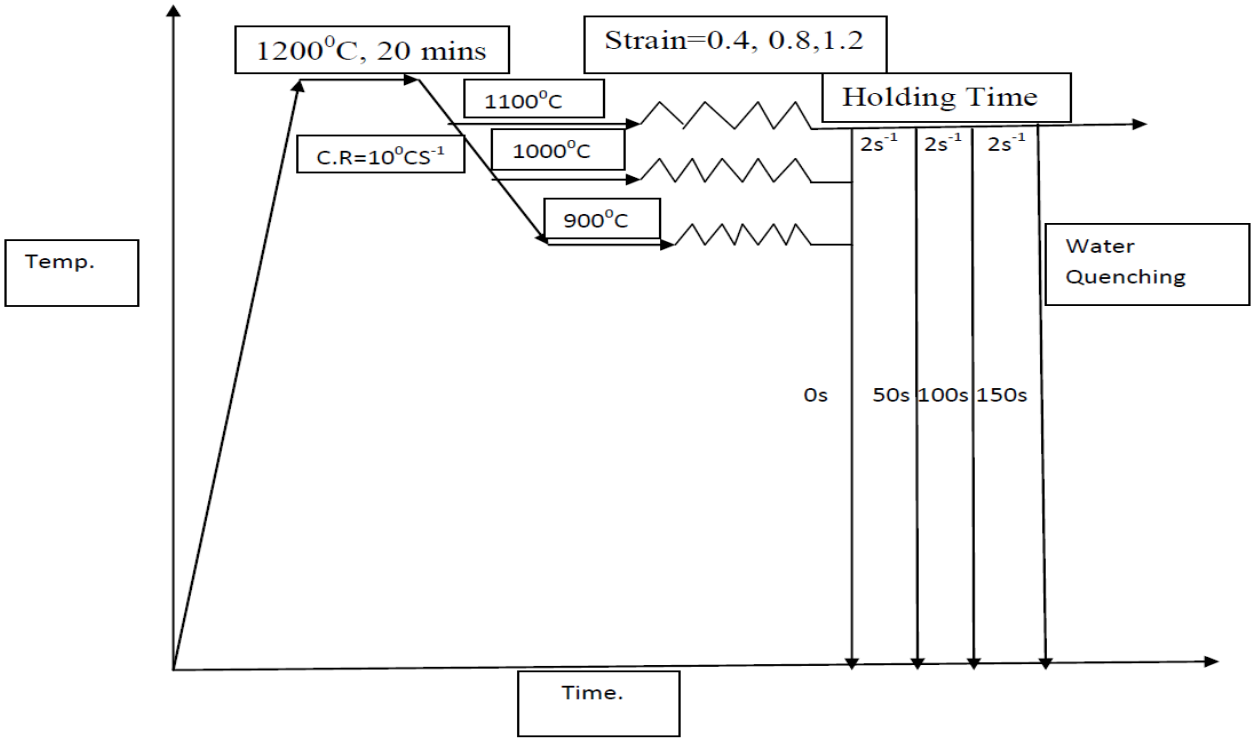

Figure 3.1 Schematic view of TMP schedule.

Table 3.2

Experimental parameter for Hot deformation study

Reheat temp(^{0}C)&Time(min)	Strain rate (s^{-1})	Temp(C^0)	Strain	Cooling Conditions
1200^{0}C&20mins	2	900^{0}C	0.4,0.8,1.2.	Water- quench
1200^{0}C&20mins	2	1000^{0}C	0.4,0.8,1.2.	Water- -quench
1200^{0}C&20mins	2	1100^{0}C	0.4,0.8,1.2.	Water- quench

3.3 Characterization of the Specimen

The detailed micro structural characterization of the deformed specimens was proceed out with a presence of optical microscopy, scanning electron microscopy (SEM) and electron backscattered diffraction (EBSD) experiments. Standard metallographic methods were followed to prepare the samples for characterisation for Optical and SEM followed by etching while extra care is required while preparing the samples for EBSD with colloidal silica polishing.

3.3.1 Metallographic

The hot deformation processed samples for were cut along the longitudinal section to obtain the microstructures, more or less from the centre of the diameter, i.e., from the core of the deformation. The sectioned samples were then mounted in a Bakelite resin using hot mounting press. The flat mount samples were then polished using different grades of silicon carbides emery paper starting from coarser to finer sizes (320,400,600,800,100,1200 and 2000 grits) with rotating the polishing direction of sample by 90° to ensure the removal of deformation effects of previous paper polish. After completion of the emery paper polishing sequence, disc cloth polishing was carried out using fine grained alumina solution (AP-D Powder 0.05μm) until a scratch free mirror like surface. Finally, the samples were sonicated using ethanol in an ultrasonic cleaner for about 10 min, to remove any polishing debris. The grain structures were revealed by subsequent etching using 2% Nital solution, for examination under SEM and Optical microscope. For EBSD studies, instead of etching, an additional polishing was carried out for long time with OPS (colloidal silica) to obtain a very good free surface finish under there no presence of strain on the specimen.

3.3.2 Optical Microscopy

The etched specimens were examined under LEICA make LAS V3.8 metallurgical optical microscope. The optical micrographs were digitally acquired from CCD camera attached to the optical microscope and image analyses were performed on the micrographs using Image J, public domain software to obtain quantitative micro structural information.

3.3.3 SEM (Scanning Electron Microscope)

The detailed examination of microstructure at higher magnification and determination of the chemical composition by X-ray analysis was carried out in FEI Make Nova Nanosem at 20KV attached with EDAX facility. The samples prepared for Optical microscopy were examined under SEM for further analysis of micro structural information.

SEM is that type of electron microscope which is basically used for getting the surface topography and composition of the specimens. The basic principle of SEM is that when electron beam interact with the atom of the specimens then produces various signals such as X-ray, back scattered and secondary electron which are helpful for getting the clear micrographs of surface morphology. The electron beam is generally scanned in raster can pattern and the beam position is combined with detected signals to produce an image. The secondary electron which has developed when it interact with the atom at near on the surface.The main advantage of SEM is possibility of wide range of magnification is possible (i.e, 10 times larger magnification than the simple type of optical microscope) to more than 5000 times.

Figure 3.2.A schematic view of SEM.[61]

The image magnification in SEM is not the power of objective lens and it is only focus the beam to a spot with the help of condenser mainly not for getting any kind of image [61]. The magnification is a function of ratio of screen size to scan size on the sample. The electron source being field emission gun can provide strong current density with improved resolution of 2-3 nm at 20 KeV. [61]

3.3.4 EBSD (Electron Back Scattered Diffraction)

Four samples were selected based on nature of flow curves obtained from the deformation experiments and subjected to EBSD analysis to obtain the detailed micro texture and micro structural analysis. The EBSD – OIM (orientation imaging microscopy) analysis was carried out with a CCD camera acquisition of digital Kikuchi patterns using TSL-OIM data collection software attached to the FEI make Nova nanosem FEG SEM. EBSD acquisition was proceed out with step size of 0.07/1 µm with a scan size of ~ 100 µm X 100µm. The acquired data were analysed using TSL-OIM analysis software to obtain various information like grain boundary misorientation, inverse pole figure and image quality maps.

It is also known as backscattered Kikuchi diffraction, is a useful technique to identify the crystal orientation from a material surface. This technique is used for Orientation Imaging Microscopy (OIM).The EBSD technique relies on positioning of a specimen within a scanning electron microscope (SEM) chamber such that the angle between sample surface and focussing electron beam is approximately 20^0 (Figure 3.1).When the sample surface is tilting with respect to incident beam, then angle between them is 70^0 degree (under considering the normal surface).An screen is placed in front of the sample for getting the image by capturing

the back scattered . The screen is coated with a fine grained phosphor such that its luminescence spectral peak matches the response of the CCD camera used to image it.

3.3.4.1 Kikuchi Pattern Formation and Analysis:

As the primary electrons enter a crystalline solid, they are diffusely and incoherently scattered in all directions. These scattered electrons may impinge on crystal planes at The Bragg angle (θ).Since diffraction of the elastically scattered electrons through Bragg angle is occurring in all directions, it result in a cone which extends about the normal of the reflecting atomic planes with half apex angle 90^0-θ.Each family of planes gives rise to two cones, one from either side of the imaginary source. The Bragg angle, for typical values of the electron wavelength and lattice interplanar spacing, is found to be about 0.5^0.

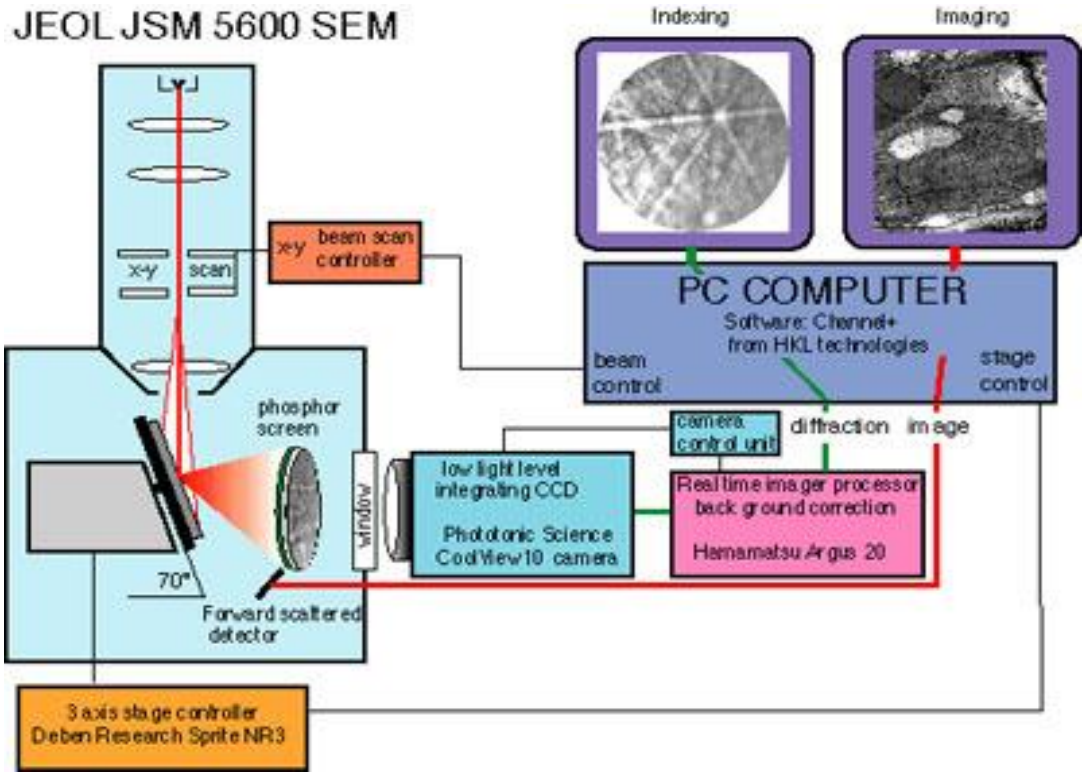

Figure 3.3. Typical OIM/EBSD attachment in SEM.[62]

Consequently, the apex angle of a diffraction cone is close to 180^0, i.e the cones are almost flat. When the phosphor screen intercepts the diffractions cones, a pair of parallel conic sections results, which appear to be parallel lines (refer Fig. 3.2).These are called Kikuchi lines.

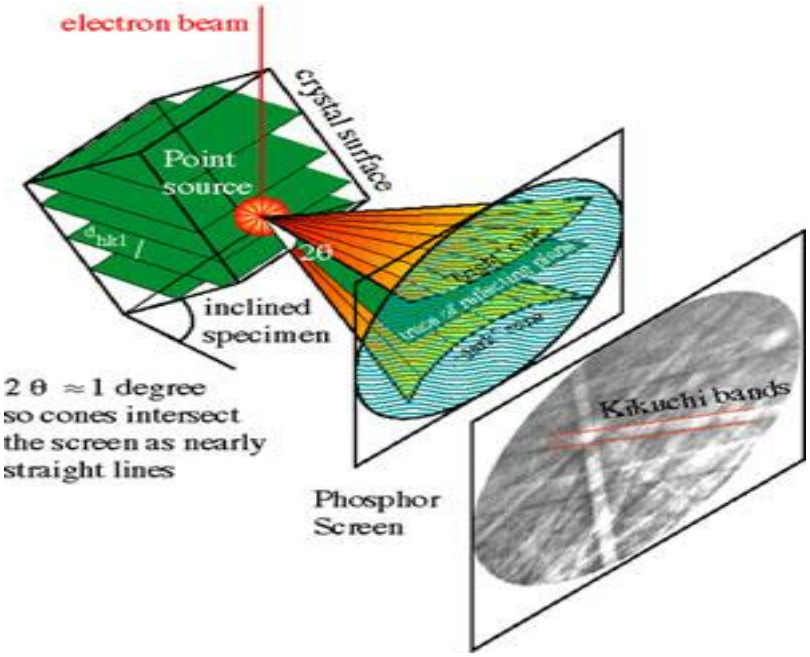

Figure 3.4: Inelastic scattered electrons from specimen generating Kikuchi-lines on Phosphor Screen [62].

The whole EBSD kikuchi pattern consists of pairs of parallel lines where each pair is known as a Kikuchi band. It has a distinct width and corresponds to a zone axis (pole).The kikuchi pattern therefore essentially embodies all the angular relationships in a crystal, both the interzonal and interplanner angles are present, and therefore implicitly contain the crystal symmetry. Commercial automated system attempt to determine the orientation based on the geometrical arrangement of bands in the kikuchi pattern. Therefore, the first step in automated indexing of EBSD is to extract the bands from the pattern. Krieger Lassen etal.First suggested using the Hough transform to extract band information. This has proven to be in general robust method and is therefore most commonly employed today.

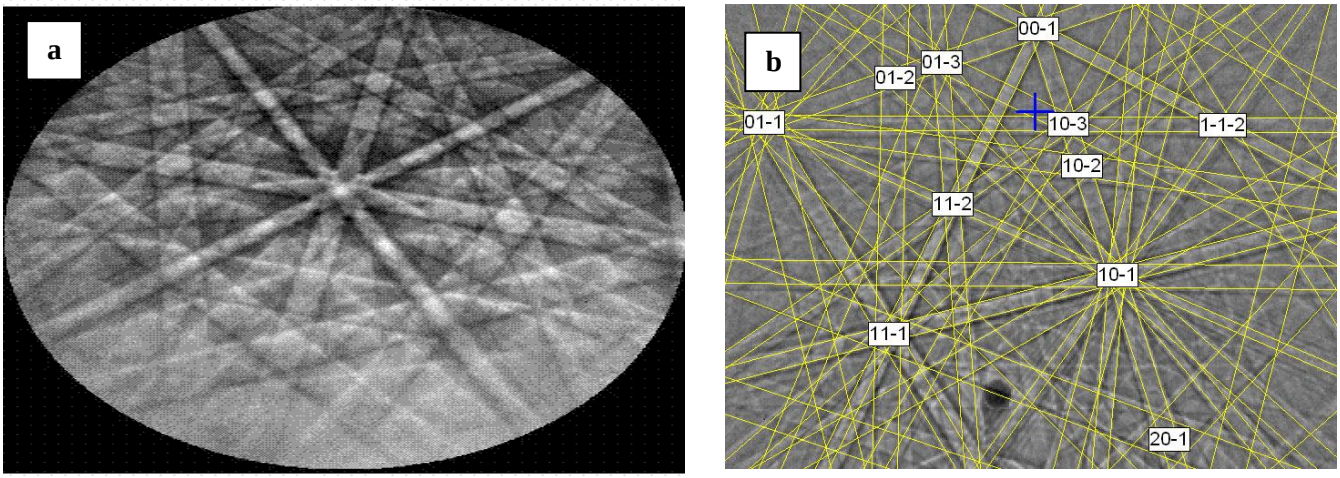

Figure 3.5(a) A kikuchi pattern (left) is transformed to Hough space (middle) where single high intensity peak are detected.(b) Indexed pattern showing crystal orientation defined by Euler angles.[63]

.

The equation governing the Hough transform is

$$\rho = x \cos\theta + y \sin\theta$$

Where (x,y) describe a set of pixel coordinates forming a line and the Hough parameters (ρ,θ) provide a wave like functions in Hough space. As the intensity of each (x,y) pixel is added, the problem of finding a kikuchi band is now reduced in finding a peak of relatively high intensity in the Hough transform.

Once the bands have been detected, the reflecting planes associated with the detected bands must be identified. Two band characteristics can be used for indexing; (1) the width of a band, which is a direct function of the d-spacing through Bragg's law, this option is a power tool for improved accuracy dealing with structures of low symmetry and for phase identifications. (2) The angle between the (located) bands which are known and compared to a theoretical directory of interplannar angles; this standard method used in TSL software.

Selection of the most likely indexing solution for automated system is to use a voting scheme. Each time the angles in a triplet of bands are compared to the look-up table allowing the miller indices (hkl) associated with the bands to be identified. All possible solutions within the tolerance angle are registered for any triplet and each solution yields a vote. The most probable solution is the one that receives the majority of votes. In order to assess the reliability of the indexing, several parameters such as the image quality (IQ), the confidence index (CI) and the fit between the recalculated and the detected bands may be discerned. The IQ reviews the relative quality of the pattern using the intensities of the found Hough peaks. The CI is given by

$$CI = (V_1 - V_2) / V_{total}$$

Where V_1 and V_2 are the number of votes for the first and second solutions and V_{total} represents the total possible number of votes from the detected bands .The CI will yield a value between 0 and 1.In general, C I values higher than 0.2 will represent a proper indexed pattern [63].The fit parameter defines the average angular deviation between the recalculated and the parameters defining the crystal structure.

3.3.5 Micro Hardness Testing

It was conducted for the specimen using LECIA VMHT Auto micro hardness tester .Micro hardness testing is divided into type of hardness test in which one of the test is Vickers Hardness Test. In this test consist a diamond indenter which is basically used for measuring the degree of hardness of the surface of the specimen. During indenting the specimen a load of 1 to 100kgf is used loading and right pyramid shape with square base has developed with an angle base of 136^0 between the opposite faces. The surface indentation of diamond indenter, which has left on the surface after releasing the load are measured by using a microscope and there average is calculated. The area of the sloping surface of the indentation is calculated.[60]

.

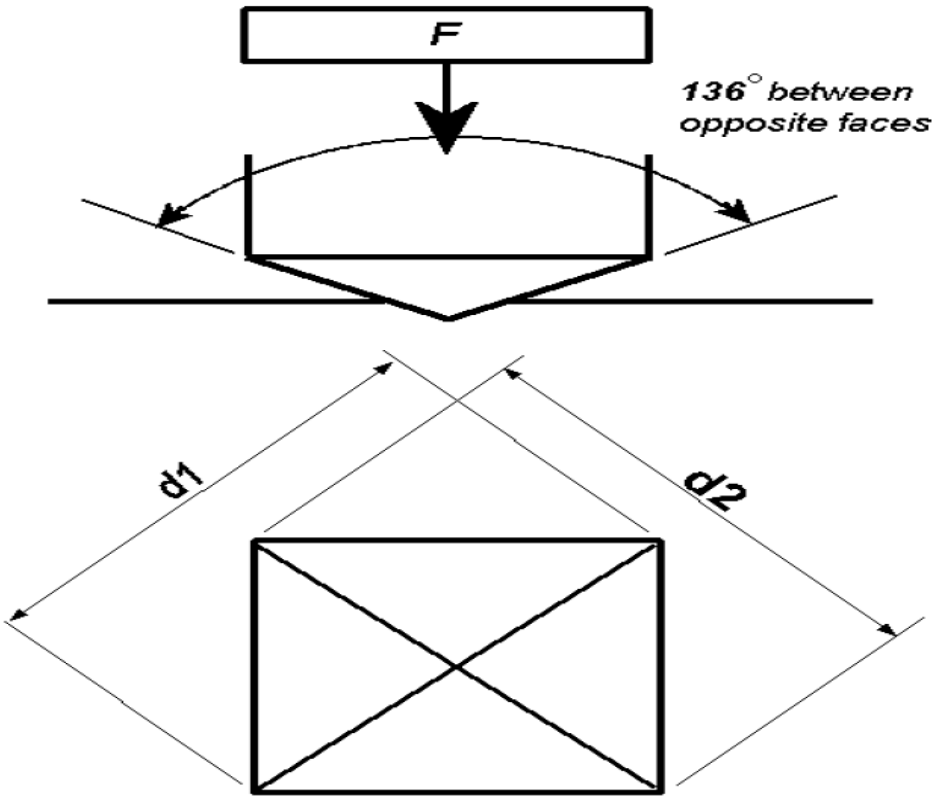

Figure 3.6 Show the schematic view of Vickers Hardness Testing.[60]

F= Load in Kgf , d= Arithmetic mean of the 2diagonal, d1 and d2 in mm .

HV= Vickers Hardness, $HV= \frac{2\,F\,SIN\,136°/2}{d^2}$ $HV = 1.854\ \frac{F}{d^2}$ (approx)

The main advantage of Vickers hardness is that:

1. For accurate and precise reading.

2. Same indenter can be used for all type surface of materials.

Before the hardness measurement the specimen was polished up to 1500 grit size emery paper to remove the oxide layer then fine polished for clear observation of indentation mark. The micro hardness test was carried with a indentations of 50gram for 15 sec at indentation rate of 30μm/s.Since the sample size were small only micro hardness measurement were carried out to understand mechanical properties.

CHAPTER NO : 04

RESULT & DISCUSSION

4.1 As received Material Characterization

In the present investigation, API X60 steel specimen of thickness 7mm was used as the starting material for the thermo-mechanical treatment. Figure 4.1 shows the optical micrographs of as received plates. The microstructure is right proportion of ferrite and pearlite in which large part is ferrite and small part of pearlite(appears dark). Fig 4.2(a) shows the SEM micrographs which clearly reveal the presence of polygonal ferrite having an average grain size ~6 μm as measured by Image J software. SEM micrograph taken at higher magnification in Fig 4.2(b), shows the alternating layers of ferrite and cementite is somewhat degenerated to the thermo mechanical processing conditions.

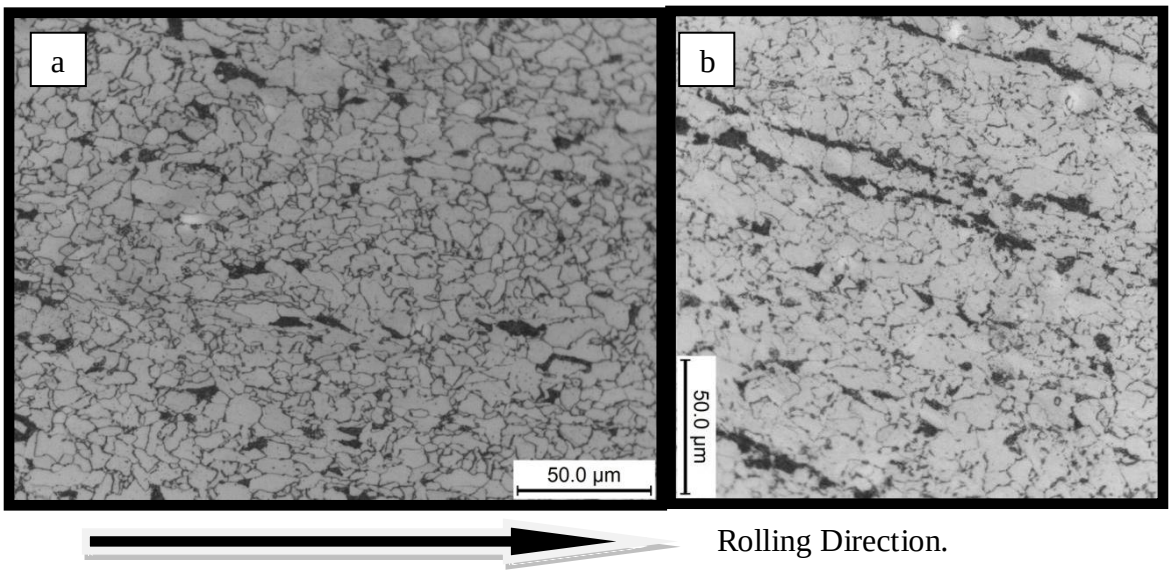

Figure 4.1: Optical micrographs of API X 60 steel plate (a) along the rolling direction (b) rolling cross-section.

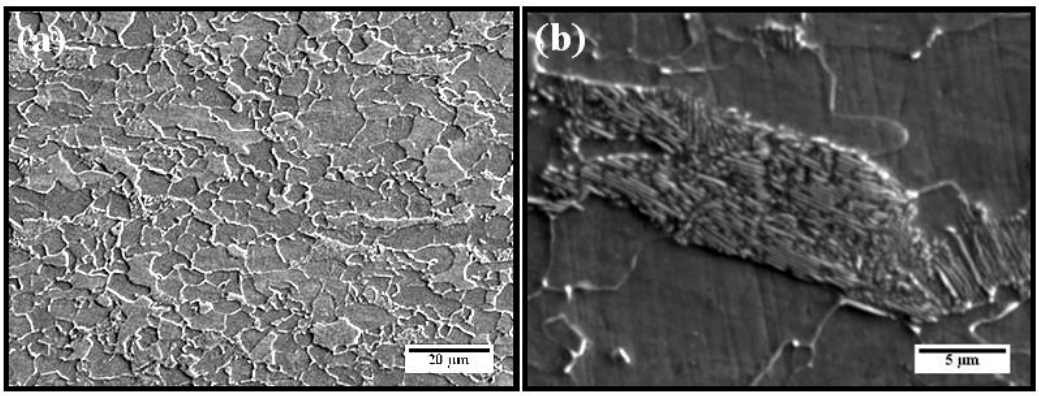

Figure 4.2 .SEM micrographs of API X60 steel plate (a) at lower magnification, (b) at higher magnification.

4.2 Thermo-mechanical Processing (Flow curves and recrystallisation mechanism)

In the present approach, high temperature compression tests was carried out under different deformation temperature such as 900^0C, 1000^0C and 1100^0C for different strain levels 0.4, 0.8 and 1.2 at a constant strain rate 2 s^{-1}. The experiments were conducted by using the DIL805D type deformation dilatometer. The flow curves which based upon the above test are basically used for examine the deformation behaviour and nature of recrystallisation conditions which govern the flow behaviour.

The stress-strain curve in a continuous manner has plotted under following the all above mentioned deformation conditions for API X-60 steel which are shown in figure (4.3).It is can easily monitor from the stress-strain curve that increment in flow stress value cause decrement in all deformation temperature. This can be reasoned such that softening due to recovery and recrystallisation kinetics decrease with lagging in the deformation temperature. From, the stress-strain flow curve, the critical and peak value of stress and strain is clearly indicated. From the figures, it clearly indicates that similarity between the all the curves under different deformation temperature with fixed strain rate. This indicates that the reliability of performing the experiments in the deformation dilatometer.

Considering the evolution of microstructure during TMP, the flow curve can be successively divided into three stages. During the initial stage of low strain (i.e., at 0.4), the work hardening and dynamic recovery behaviour has occurred and this state is basically characterised by process name which is known as static recrystallisation in which deformed grains are elongated in particular direction as such manner which is called “pancake” microstructure. The second stage at which strain (greater than 1), the final microstructure became equiaxed and which has followed by steady state regime. Both above stage are separated by another stage which is known as transition zone in which there is drop in the value of stress and this is basically indicates the onset of dynamic recrystallisation .There no formation of peak in the flow curve who deformed at 900^0C and 1000^0C and it only show the dynamic recovery which increase with increment of strain.

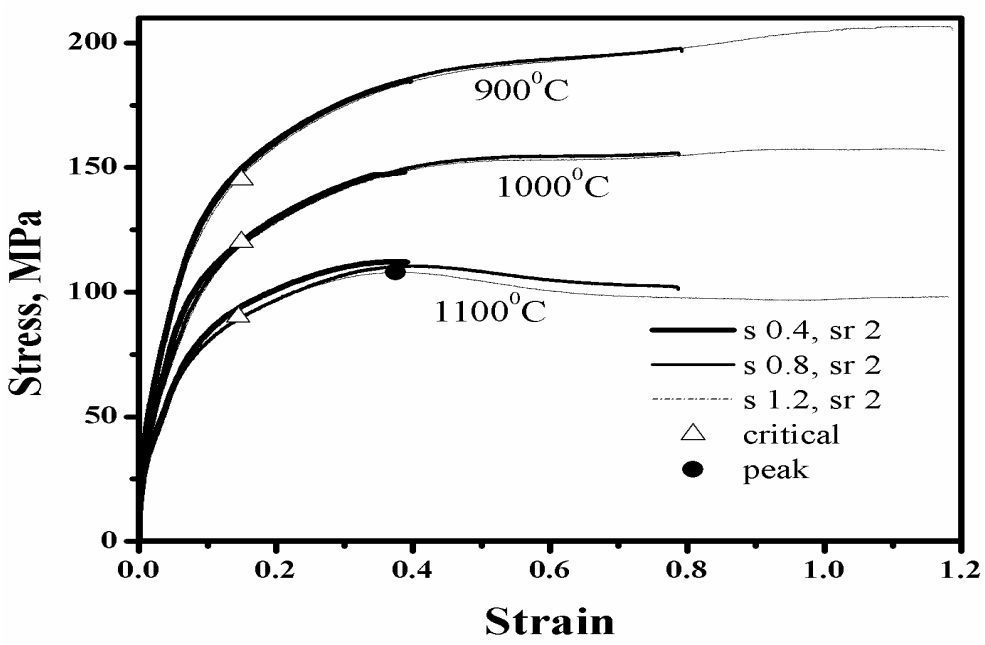

Figure 4.3: Flow curves of the API X60 Steel for all the different deformation condition.

The role of critical strain is very vital for indicating the initiation of DRX.According to Ryan and Macqueen [69], the definition of critical strain has defined as the strain where experimental flow curves deviates from the ideal behaviour of dynamic recovery. There is an alternative method in which is aimed to plot θ x stress VS stress^2 then by using this we can easily judge that how the flow curve is affected by the initiation of DRX in more precise manner. [70-73].

The differentiation of true stress w.r.t. true strain yields work hardening rate ($\theta = d\sigma/d\varepsilon$) in the region of elastic deformation. When work hardening rate (θ) combine with stress and is plotted with respect to stress^2, then point of inflection with maximum slope is basically indicates the initiation of dynamic recrystallisation.This method is facing the problems of short range noise of hinderers .For eliminating this hinderers and making the curve smooth we fit the curve in higher order of polynomial such as 8th by using "Origin Software". The detail regarding to work hardening curves w.r.t. stress has described below. Initially, the elastic region has eliminated by using the "2%" offset of total strain and after eliminating the region before the yield point then fitted the curve into higher order of polynomial for making the curve smooth and hinder free because this smoothing curve is playing very important role for making the result more precise and accurate.

Here curves consist three parts in which the first part of curves has shown the decrement of θ x stress Vs stress^2 with respect to increment of stress (it means, dislocation can easily move from one place to another

with the increment of stress), while in the second part of curve has shown that there is variation in the curve shape which basically indicates the initiation of DRX. Under considering the dynamic recrystallisation behaviour, the new strain-free equaxied grain has developed and it is important to note that it actually onset at lower value of strain and stress .After achieving the stage of DRX ,the more and more softening has occurred and it is important factor for making the difference between the dynamic recovery and dynamic recrystallisation, which can easily observed from the work hardening plot at higher temperatures such as 1100°C and 1000°C, the curve loops back as shown in figure 4.4. In the third part of the flow curve only dynamic recovery has occurred which basically represent the dynamic recovery (i.e. the removal and rearrangement of defects such as dislocation in their crystal structure).

Here, the term σ_{sat} which is indicated in the figure 4.4, which represent that saturation of dislocation in the most work hardened grains and for this required amount of driving force is needed for continuation of DRX.For the calculation of the value of σ_{sat} & σ_C then first order of stress-strain curve has analyzed in which θ x stress Vs stress^2 were prepared and which are shown in figure 4.5.The term σ_C which is called critical stress which has calculated by differentiating the first order of stress- strain at which $d^2(\theta \times \sigma)/d(\sigma)^2$ is equal to zero. Once the value of σ_C is determine, then its corresponding strain has calculated from simple stress-strain curve .It is important to note that the absence of peak stress in any flow curve then it does not mean that there no presence of DRX [74-75].When there inflection between θ x stress Vs stress^2 then there at least some DRX is present.

It is an indication of peak value when specimen deformed at 1100^0 C and for all other deformation tests shown in Table 4.1.It is observed that there no formation of peak stress& strain in all other deformation conditions which are shown in table 4.1.It is beyyer to contact for getting the value of critical stress and strain for all similar conditions. As expected, critical stress decreases with increase in deformation temperature. It is interesting to note that there is little variation in critical strain with temperature. However; it is difficult to obtain any particular trend in variation of critical strain with temperature from the present study.

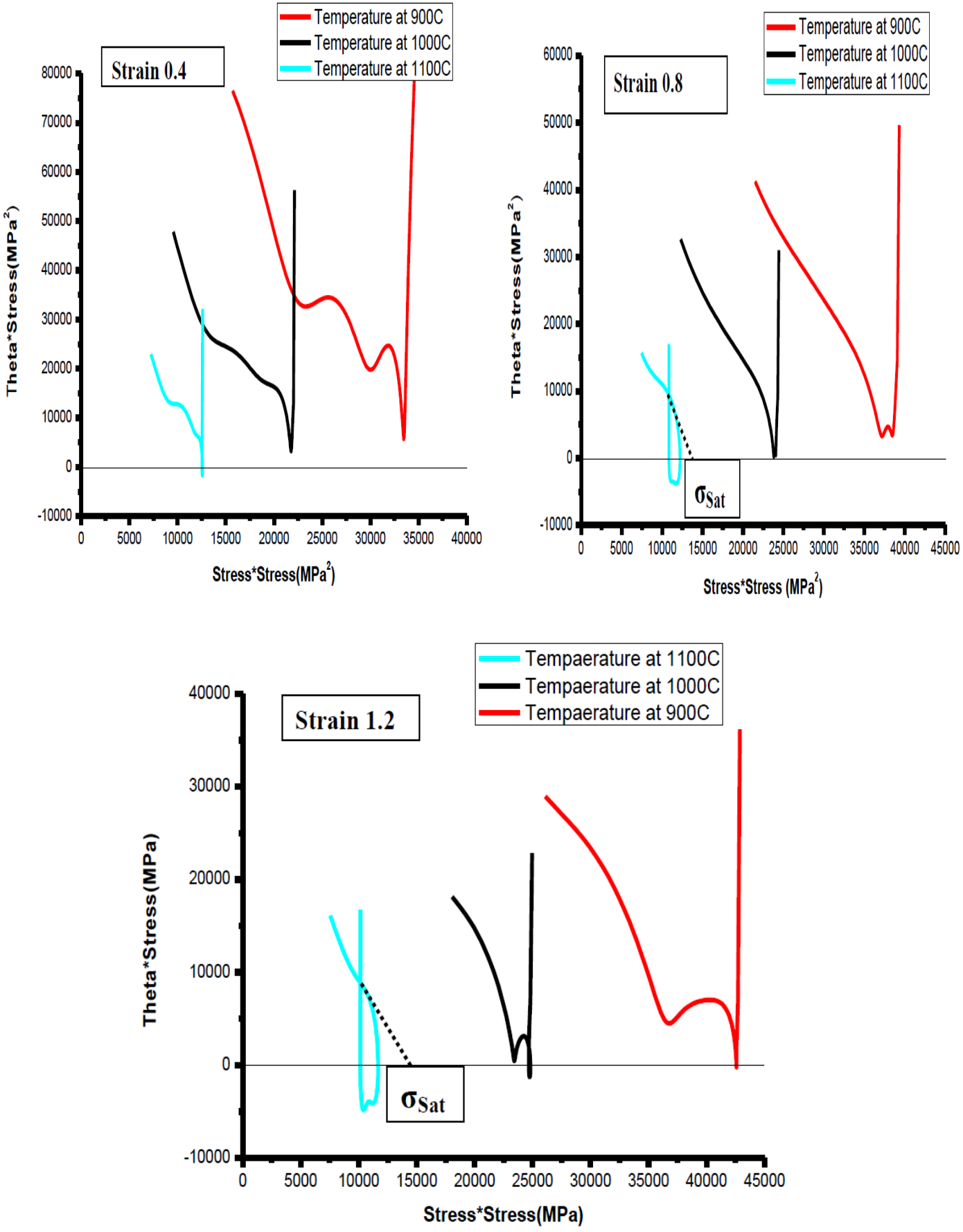

Figure 4.4. Work hardening curve of the specimen under all deformation conditions.

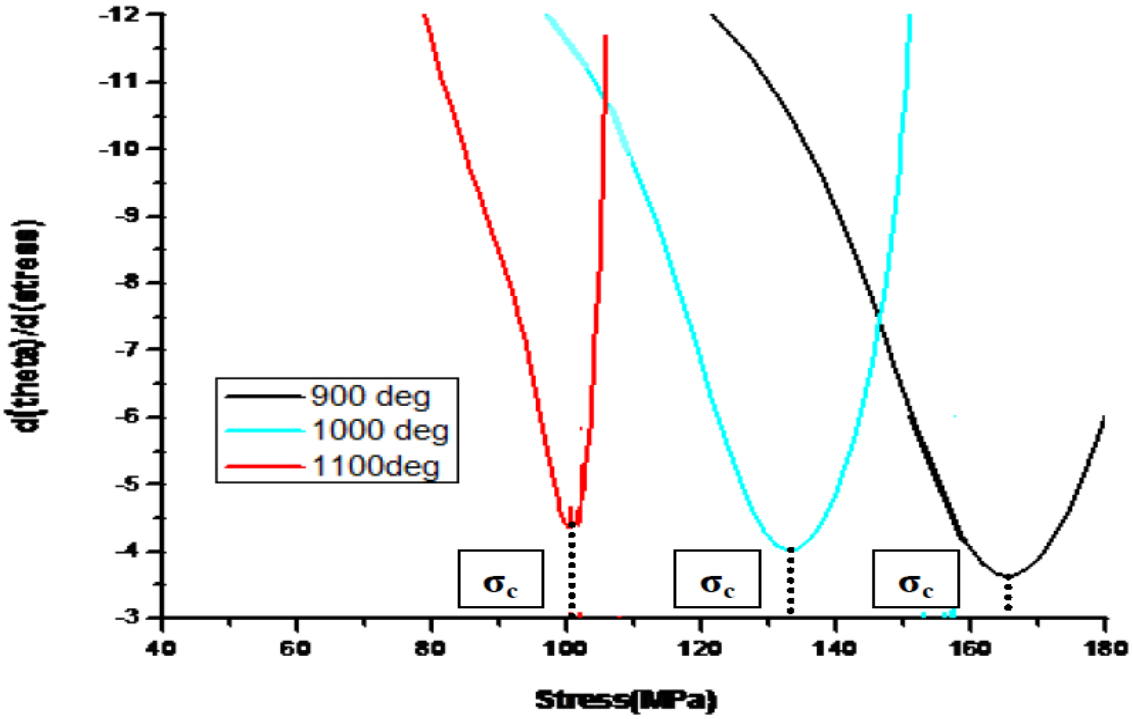

Figure 4.5: The 2nd Order derivative of the θ-σ plot (for 1.2 strain) and the minimum represents critical point (σ_c).

Table 4.1 The estimated critical stress and strain value for all high temperature deformation Tests.

Experimental strain	0.4		0.8		1.2	
Deformation Temperature (^{0}C)	Critical Stress(MPa)	Critical Strain	Critical Stress(MPa)	Critical Strain	Critical Stress(MPa)	Critical Strain
900	145	0.12	175	0.28	165	0.24
1000	110	0.108	141	0.29	133	0.234
1100	90	0.125	97	0.20	100	0.232

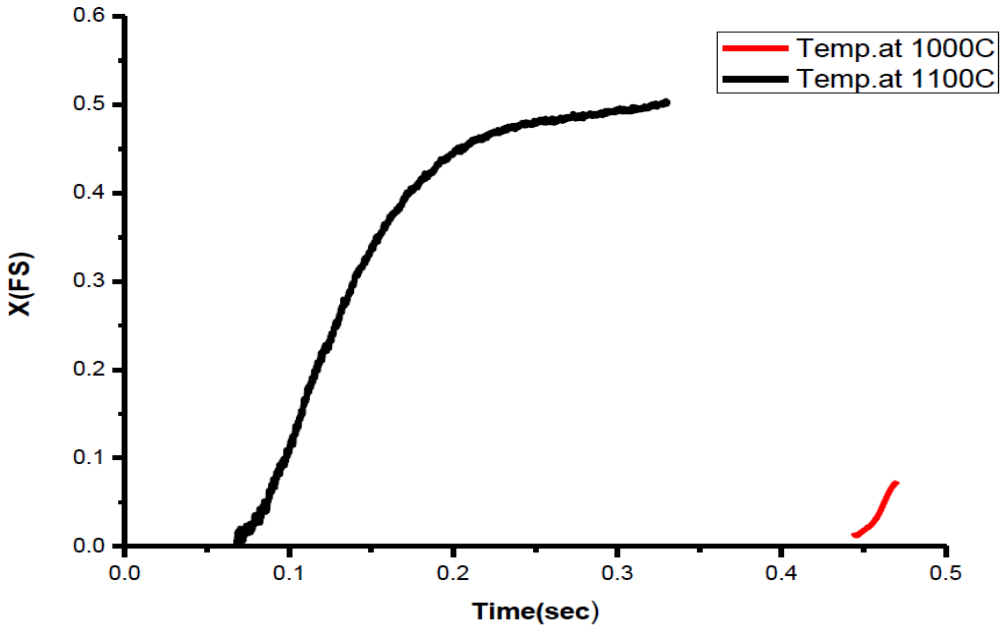

Figure 4.6 Fraction of recrystallised volume at different temperature with respect to time.

The volume of recrystallised fraction (i.e. how much fraction the grain has recrystallised) at point when slope $\theta = \delta\sigma/\delta\varepsilon$ falls to zero (critical stress) and it basically depend upon the difference between DRX and dynamic recovery.From the figure (2.9 b) it is clearly known that $\Delta\sigma_s$ is mainly responsible for net softening and is basically equal to difference between two curves such as dynamic recovery and dynamic recrystallisation curves . The maximum value of $\Delta\sigma_s$ is equal to $(\sigma_{sat}-\sigma_{ss})$, where σ_{ss} is the steady state stress under DRX conditions. The fractional softening in each case is expressed as $X = (\sigma_p-\sigma_{ss})/ (\sigma_{sat}-\sigma_{ss})$.It is important to point out that higher values of X(FS) is mainly indicates the grain structures which are associated with softening behaviours of internal portion of grains which play a very important role for recrystallisation therefore with highest value of driving force is requried . The fractional softening curves are shown in figure 4.6. This indicates there is low softening (<0.1) at 1000°C and more than 0.5 at 1100°C. The micro structural observations can only verify the above assessment of flow curves by various methods.

4.3 Microstructural Observations (Optical)

Micro structural characterisation of few selected deformed specimen (samples quenched immediately after deformation) was examined using optical microscopy, scanning electron microscope (SEM) along with electron backscattered diffraction (EBSD). Figure 4.8.1, 4.8.2 and 4.8.3 shows the optical micrographs of the specimens quenched immediately after compression the specimen up to the level strain such as of 0.4, 0.8 and 1.2 respectively at a constant rate of 2 s^{-1} and various deformation temperatures of 900^0C, 1000^0C and 1100^0C. From the optical observations, it is clear that the samples at 900°C is fine grained and resembles acicular ferrite microstructure along with some regions of bainitic laths. While the sample deformed at 1000°C, shows larger grain structure with more bainitic lath type regions and acicular ferrite. However the samples deformed at 1100°C shows very large grain sizes with the formation of more martensite along with some bainitic laths. The effect of strain levels from 0.4 to 1.2 lead to refinement of grains only in the samples who deformed at temperature about 900°C and 1000°C and no effect on 1100°C deformed sample.

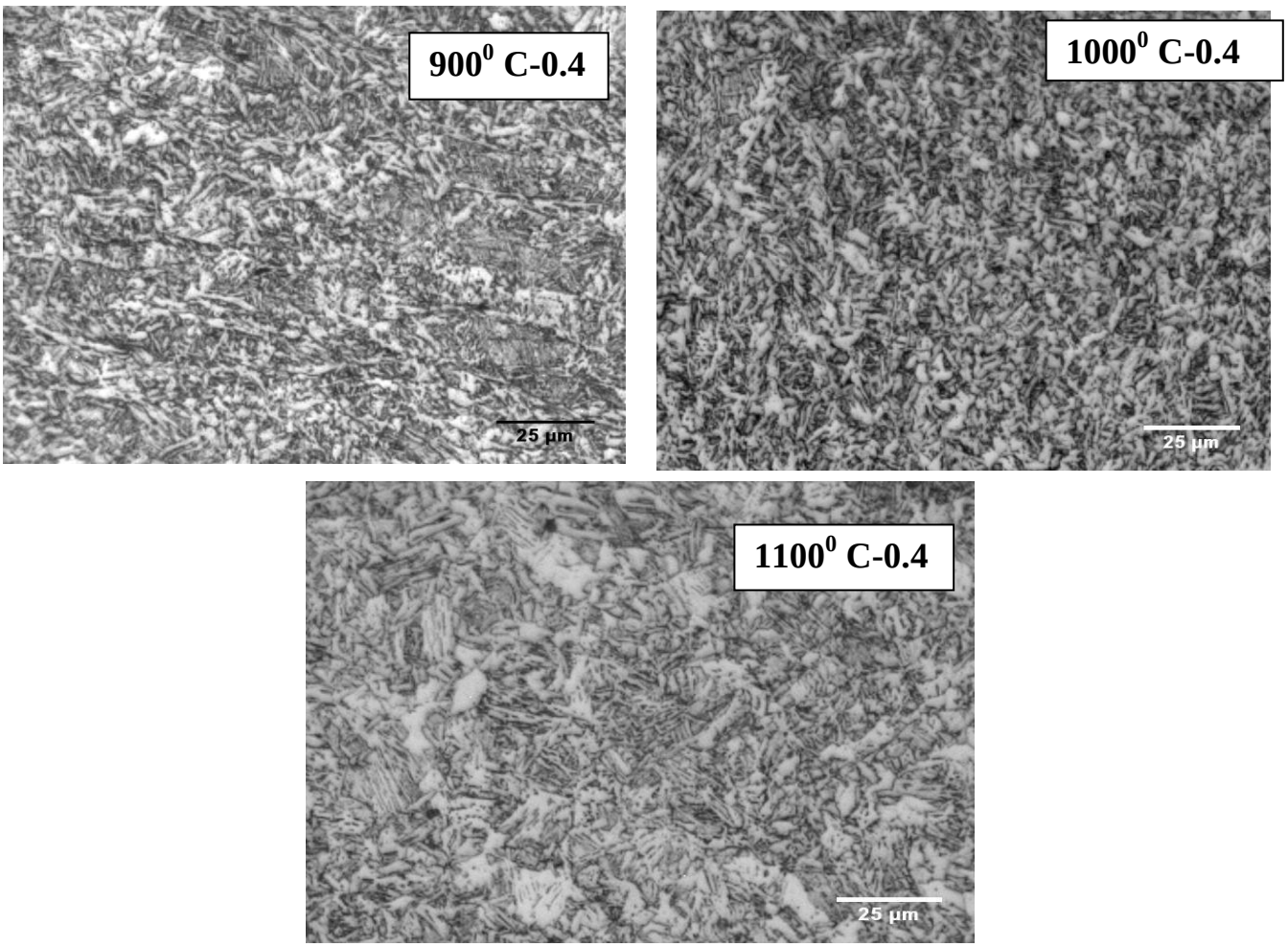

Figure 4.7 Optical micrographs of samples deformed to 0.4 true strain.

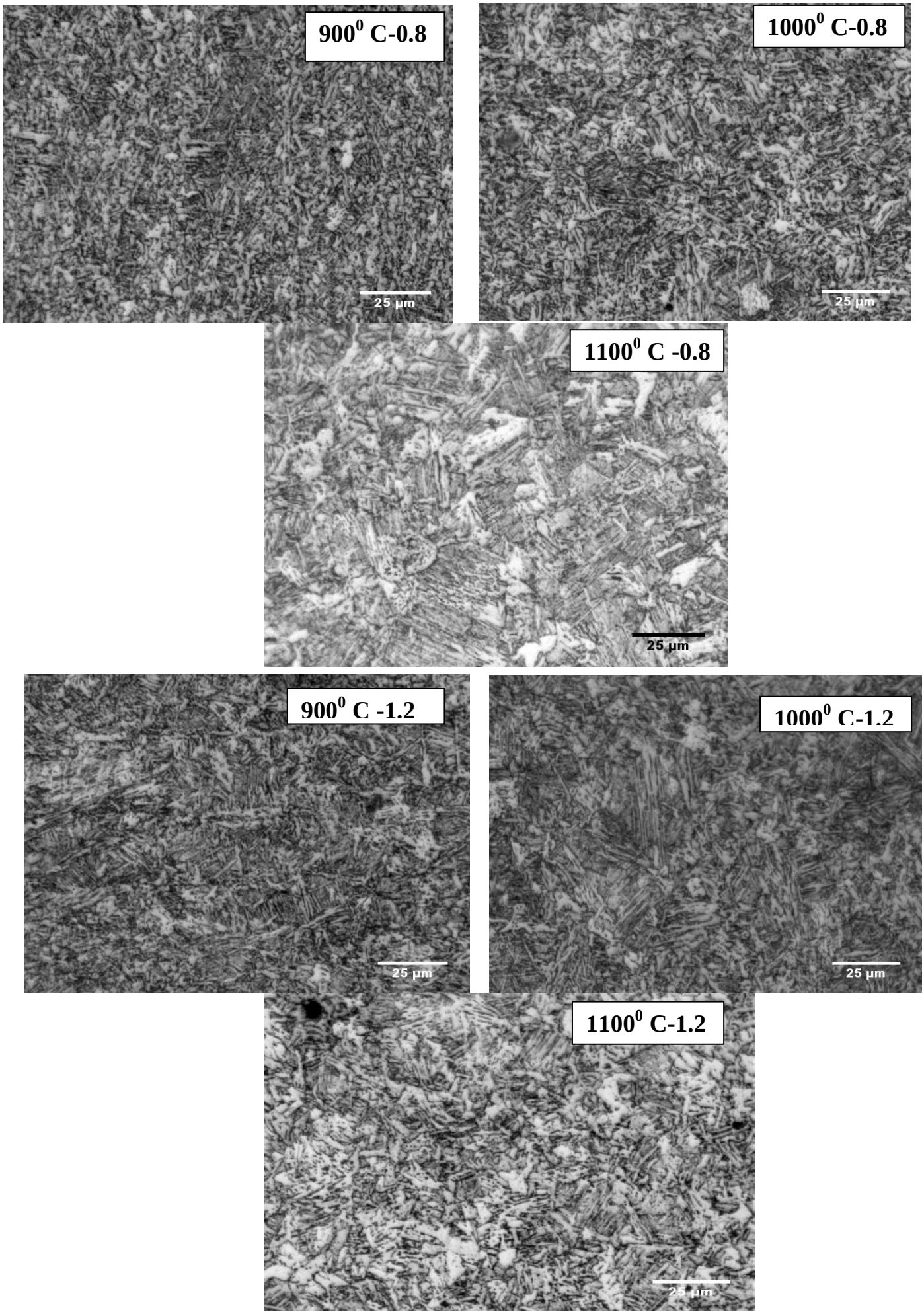

Figure 4.8 Optical micrographs at (a) 900⁰C (b) 1000⁰C (c) 1100⁰ C to strains at 0.8&1.2.

4.4 Microstructural Observations (SEM)

The samples prepared for optical examination were also examined under SEM attached with EDS to obtain more information on the microstructure evolution at higher magnifications. The nature of inclusions present and their role in the formation of the desired microstructure was examined.

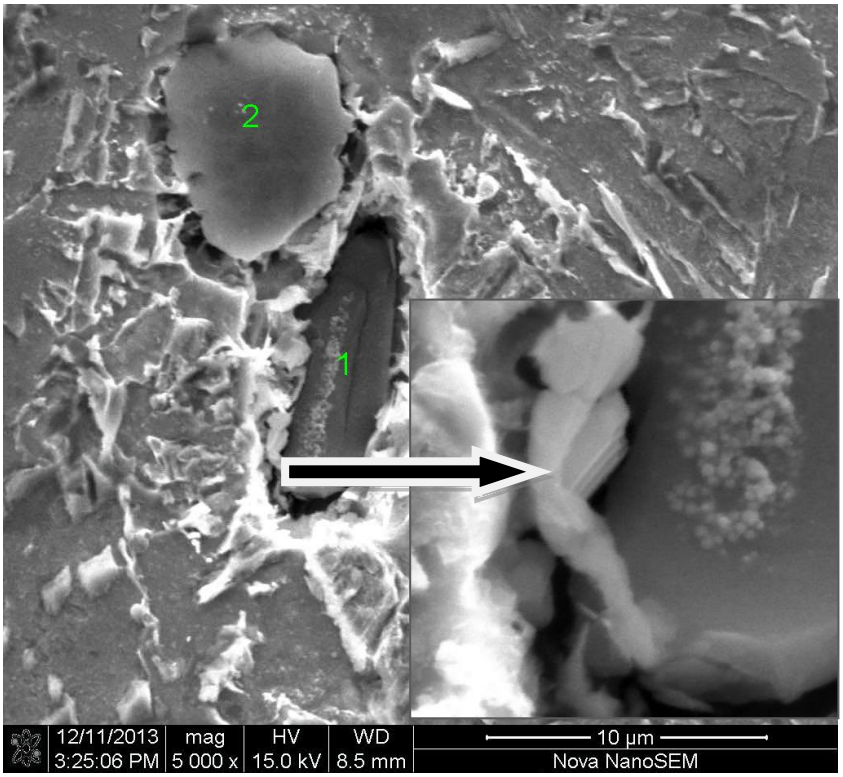

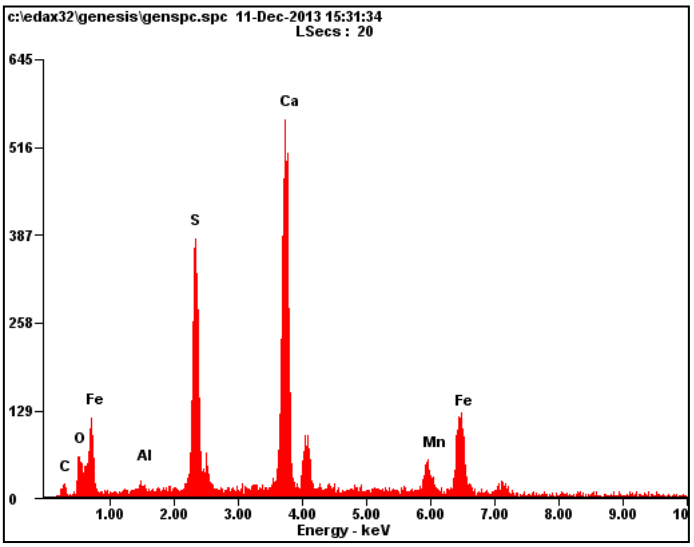

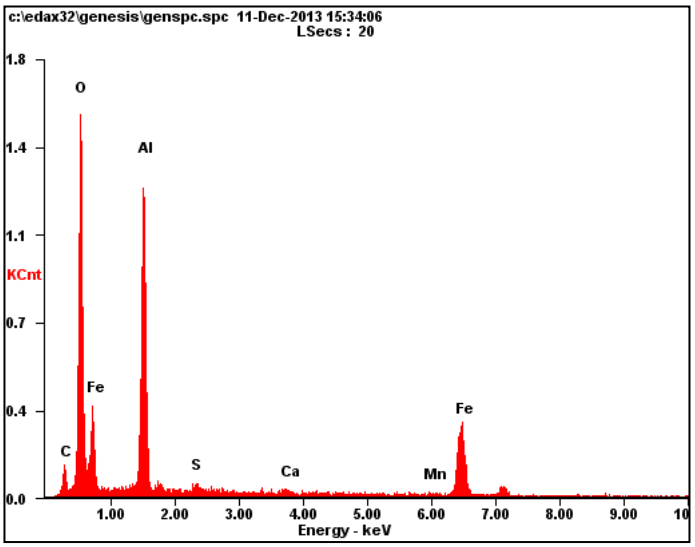

Figure 4.9 SEM micrograph showing inclusion in the API- X60 steel (at 1000° C) with inset showing bainite plates nucleating from the CaS inclusion at higher magnification along with X-ray spectrum showing the chemical constituents of inclusions.

The above micrograph shows the formation of bainitic plates in the form of lamellae at the surface of calcium sulphide inclusion. The calcium sulphide inclusion may be formed due to the addition of Calcium based innoculant to modify the elongated MnS inclusions of the microalloyed steel. The elongated inclusion i.e., MnS stringers are detrimental as they are prone to longitudinal tearing as they tend to be aligned along

the rolling direction. The presence of inclusions can also serve as source on intragranular nucleation of bainitic ferrite plates which can result in the formation of acicular ferrite microstructure.

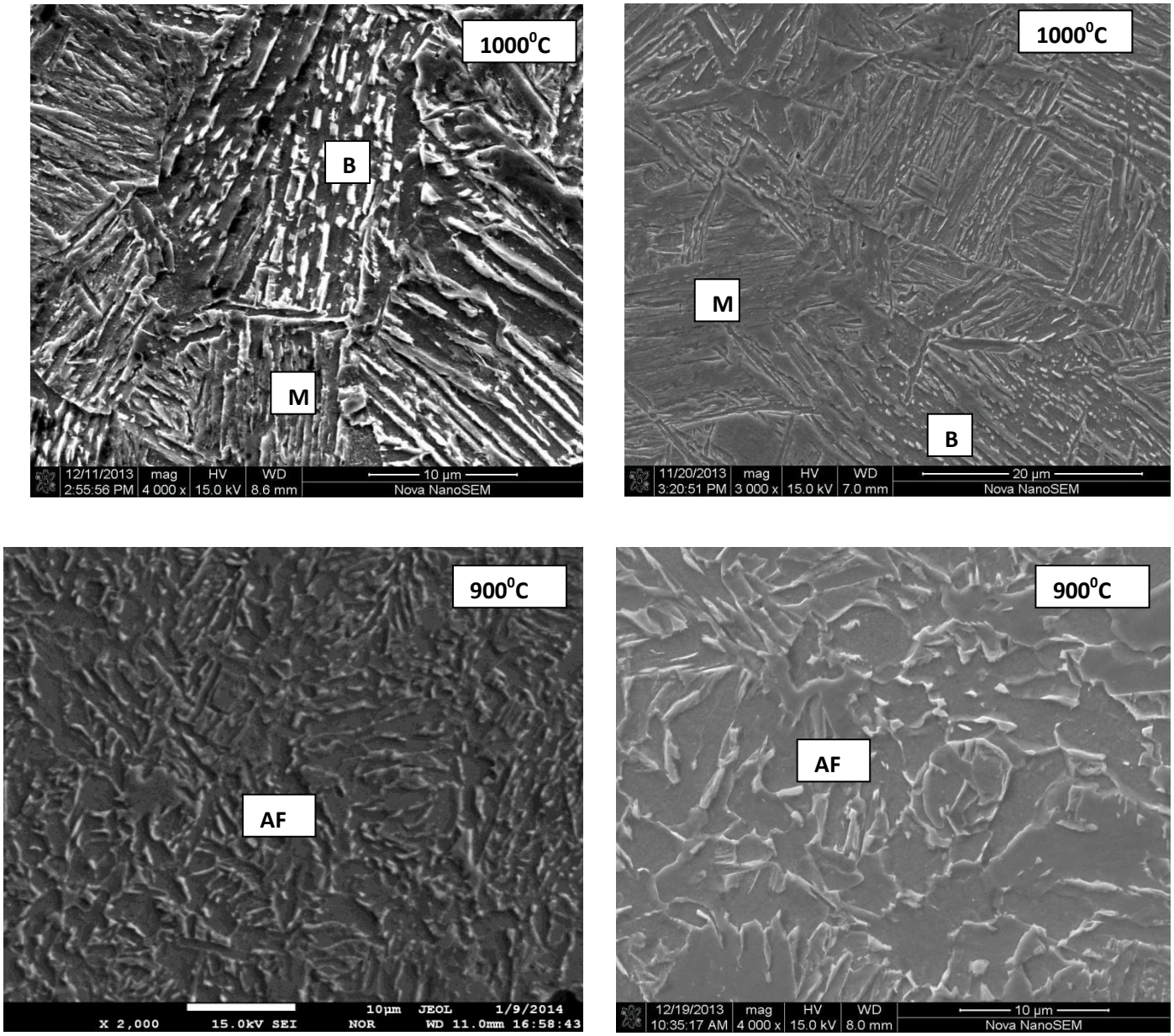

Figure 4.10 SEM micrograph showing microstructures obtained for processing at different temperatures (AF =acicular ferrite; B=bainitic ferrite; Martensite).

From the above micrograph, it is clear that the samples cooled from 900°C resulted in the form of acicular ferrite while cooling from 1000°C & 1100°C, resulted in the formation of mixed microstructure of bainite and martensite . The lower undercooling defect due to lower temperature of deformation(900°C) resulted in the formation of acicular ferrite. It is also to be noted that the deformation at this temperature may result in large intragranular high energy sites in the form of dislocation tangles and also Nb precipitation in large amounts may also act as sites for intragranular nucleation of acicular ferrite. The grain sizes are finer as

there is no softening effect, as observed from the flow curves. The large undercooling of samples deformed at 1100°C resulted in the formation of coarse grained martensite.

4.5 Microtexture Observations (EBSD)

In order to understand the microtexture evolution during the thermo mechanical processing, OIM analysis was performed on few selective deformed specimens. The objective is to understand the grain orientation and substructure especially after the critical strain levels (i.e., strain level of 0.8 for all the temperatures and 0.4 strains for 1100°C as peak strain was observed in the flow curve only in this temperature).

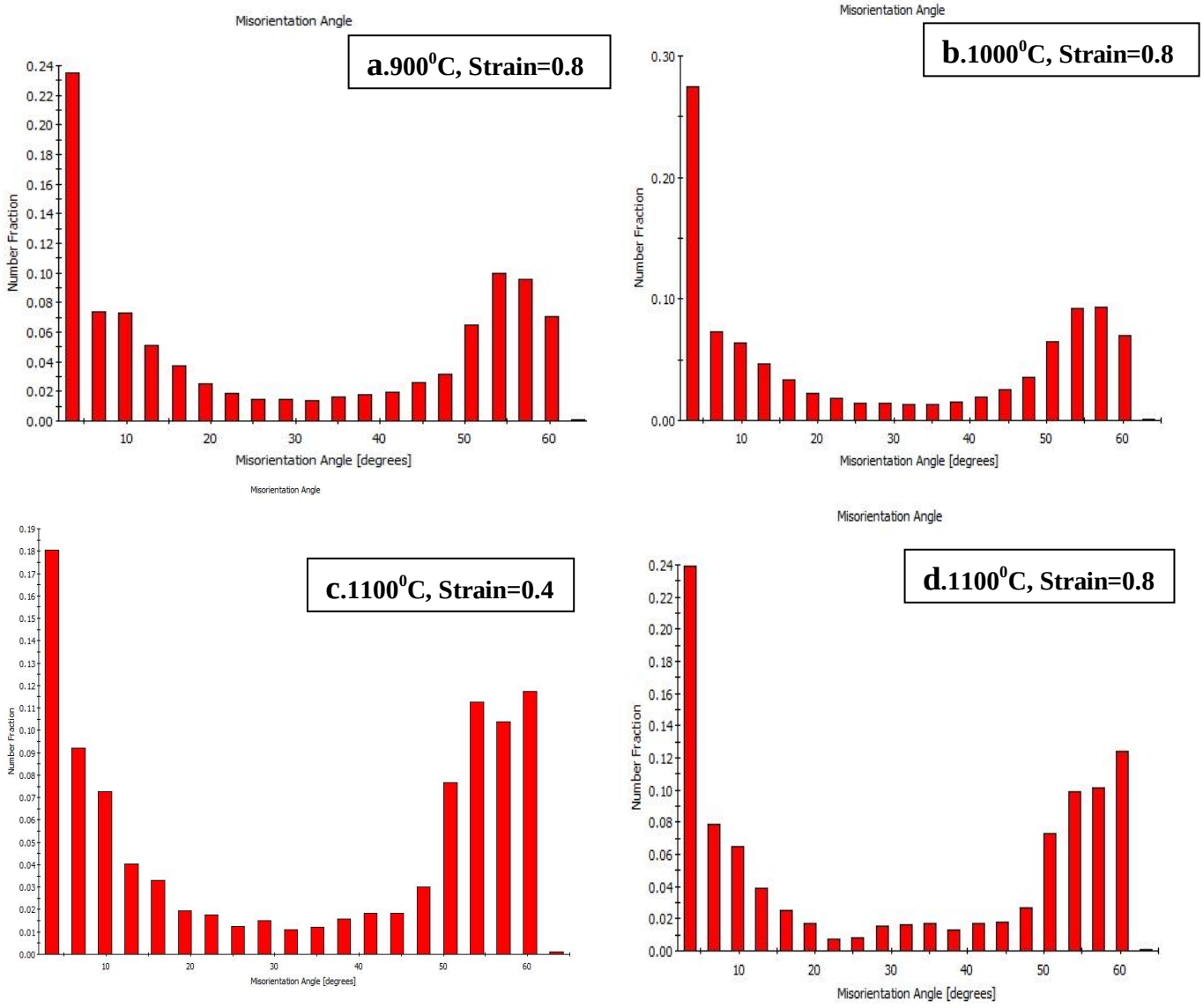

Figure 4.11 (a) to (d) Reveals the grain boundary misorientation profile for the selected samples deformed temperature of 900^{0}C (0.8 strain),1000^{0}C (0.8 strain) and 1100^{0}C (0.4 and 0.8 strain).

From the above observations, it is interesting to note that the fraction of high angle boundaries have increased with increase in deformation temperature, especially the boundaries with an average misorientation of ~60°. This implies that the fraction of recystallization grains increased with temperature, as the completed recrystallisation will lead to formation of high angle boundaries. The grain sizes were also

computed based on the changes in the orientation of the crystallites deviating more than 1°. The chart of the grain sizes for the EBSD analysed samples are shown in Fig.4.11

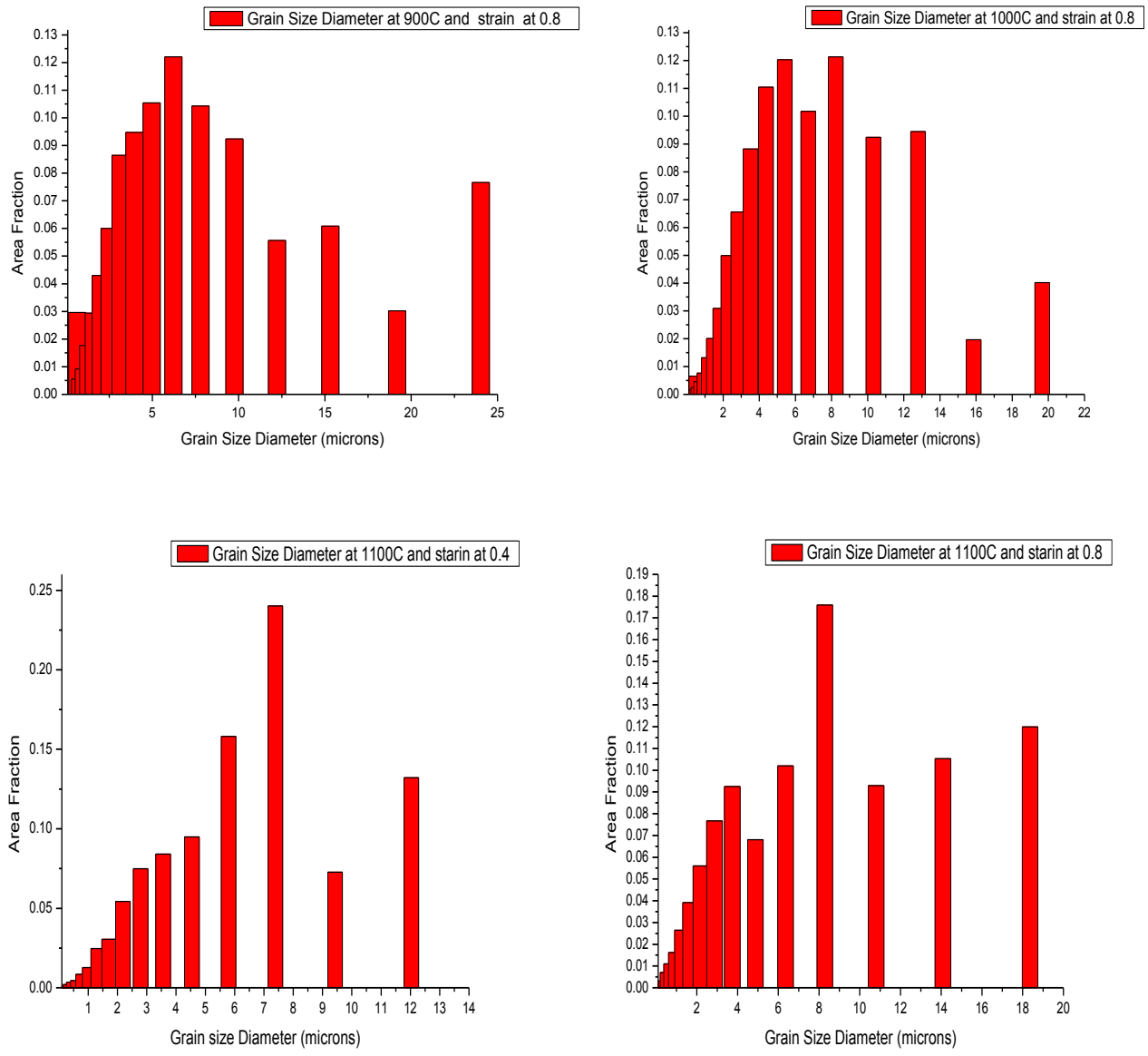

Figure 4.12. Grain size bar chart for the selected samples deformed temperature of 900^0C (0.8 strain),1000^0C (0.8 strain) and 1100^0C (0.4 and 0.8 strain).

From the above observations, it is clear that the grain sizes are very fine when the deformation was carried out 900°C increased in size with deformation temperatures at 1100°C for the same levels of strain. This indicates the softening effects were predominant at deformation temperature of 1100°C.

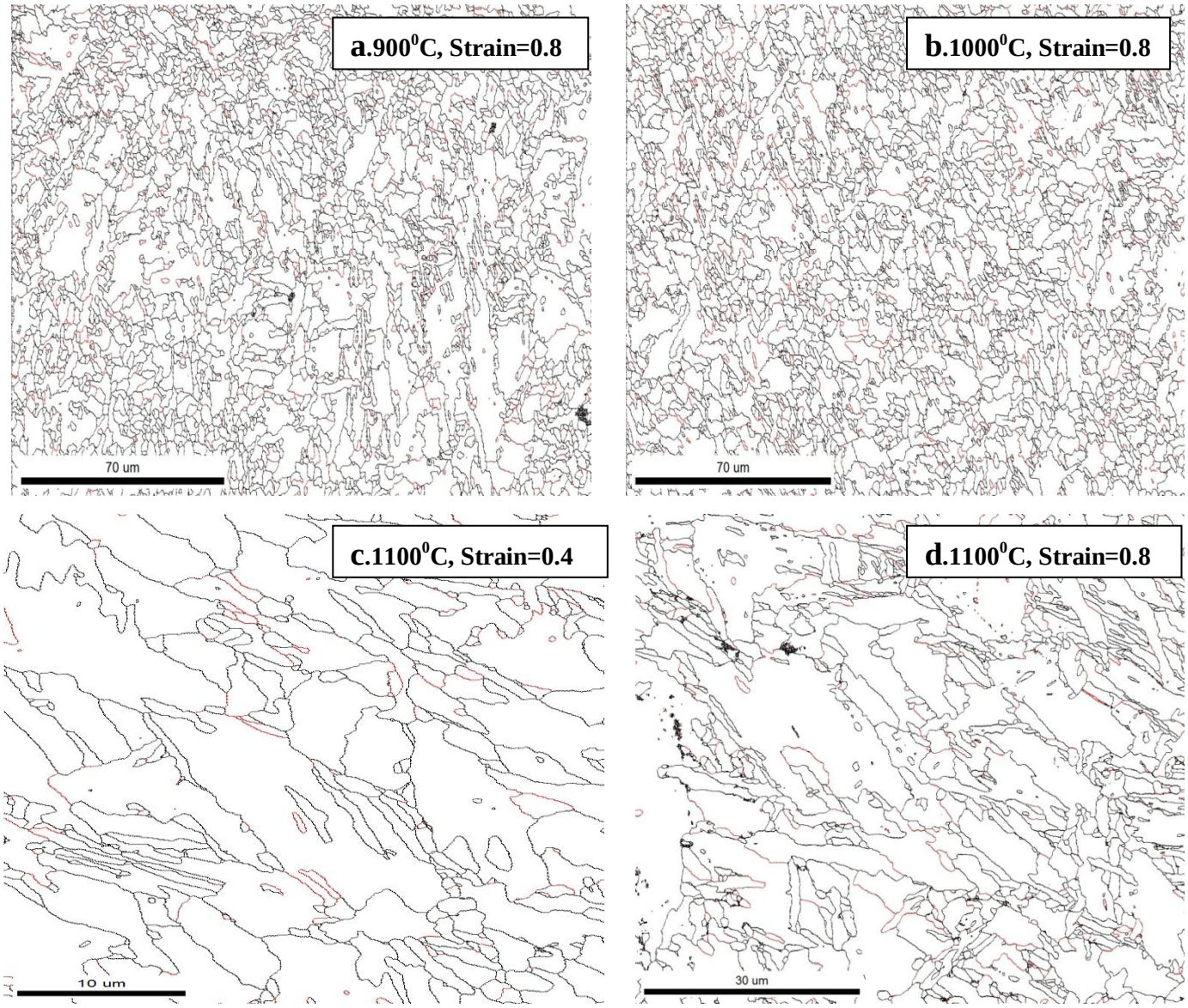

Figure 4.13. Grain boundary map for the selected samples deformed temperature of 900^{0}C (0.8 strain), 1000^{0}C (0.8 strain) and 1100^{0}C (0.4 and 0.8 strain).

From the grain boundary maps it is clear that the fraction of low angle boundaries are lower for all the deformation conditions, as the acicular ferrite formation promoted the fraction of high angle grain boundaries at the deformation temperature of 900°C while at larger temperatures, it is the effect of recrystallisation on the high angle grain boundary formation. The adjacent acicular ferrite plates nucleating intragranularly are having different orientations and hence have high angle misorientation and they are different from the aligned bainitic plates nucleating from the grain boundaries which increase low angle misorientations.

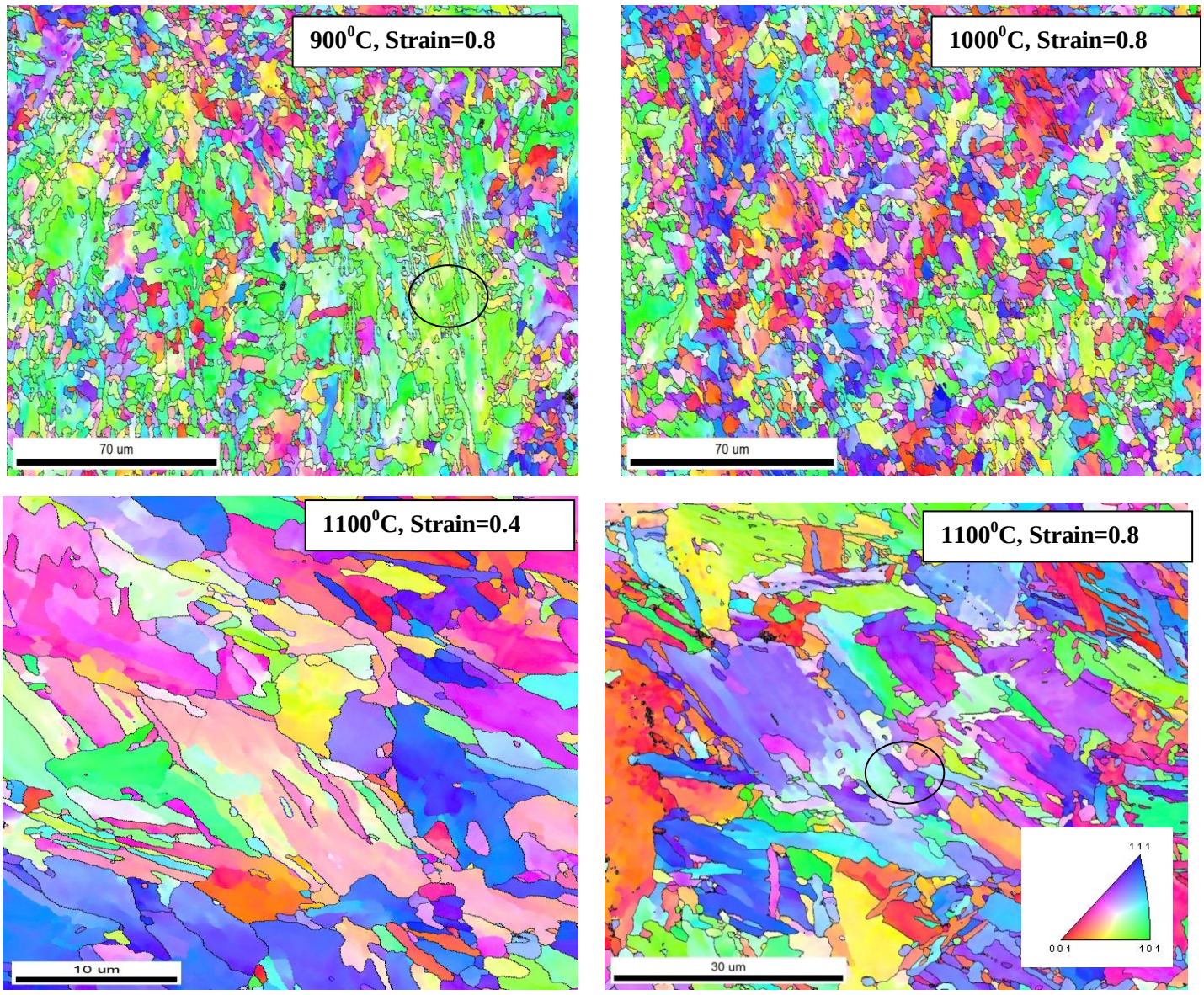

Figure 4.14. Inverse pole figure maps for the selected samples deformed temperature of 900^{0}C (0.8 strain), 1000^{0}C (0.8 strain) and 1100^{0}C (0.4 and 0.8 strain) - black circle indicates the smaller nuclei at grain interfaces.

The inverse pole figure map colour code the grains based on the orientation information and where it falls in the stereographic triangle shown above. For example, the blue colour grain indicates that the grain has orientation of (111) plane parallel to the rolling plane. The variations in colour within a grain indicate the presence of substructure with lower misorientation in that grain. The samples deformed at 900°C showed most fraction of its grains(green) has orientation parallel to the (101) crystal plane. The other orientations are favoured with increase in the deformation temperature. It is also interesting to note that tiny grains (refer to black circle in the above figure) at the interface of large grains seem to have different orientation as observed in the EBSD maps for samples deformed at 1100°C, while the tiny grains present at the interface of grains in the EBSD maps for samples deformed at 900°C are of similar orientation (yellow-green nuclei in green) supporting that the DRX occurred for samples deformed at 1100°C.

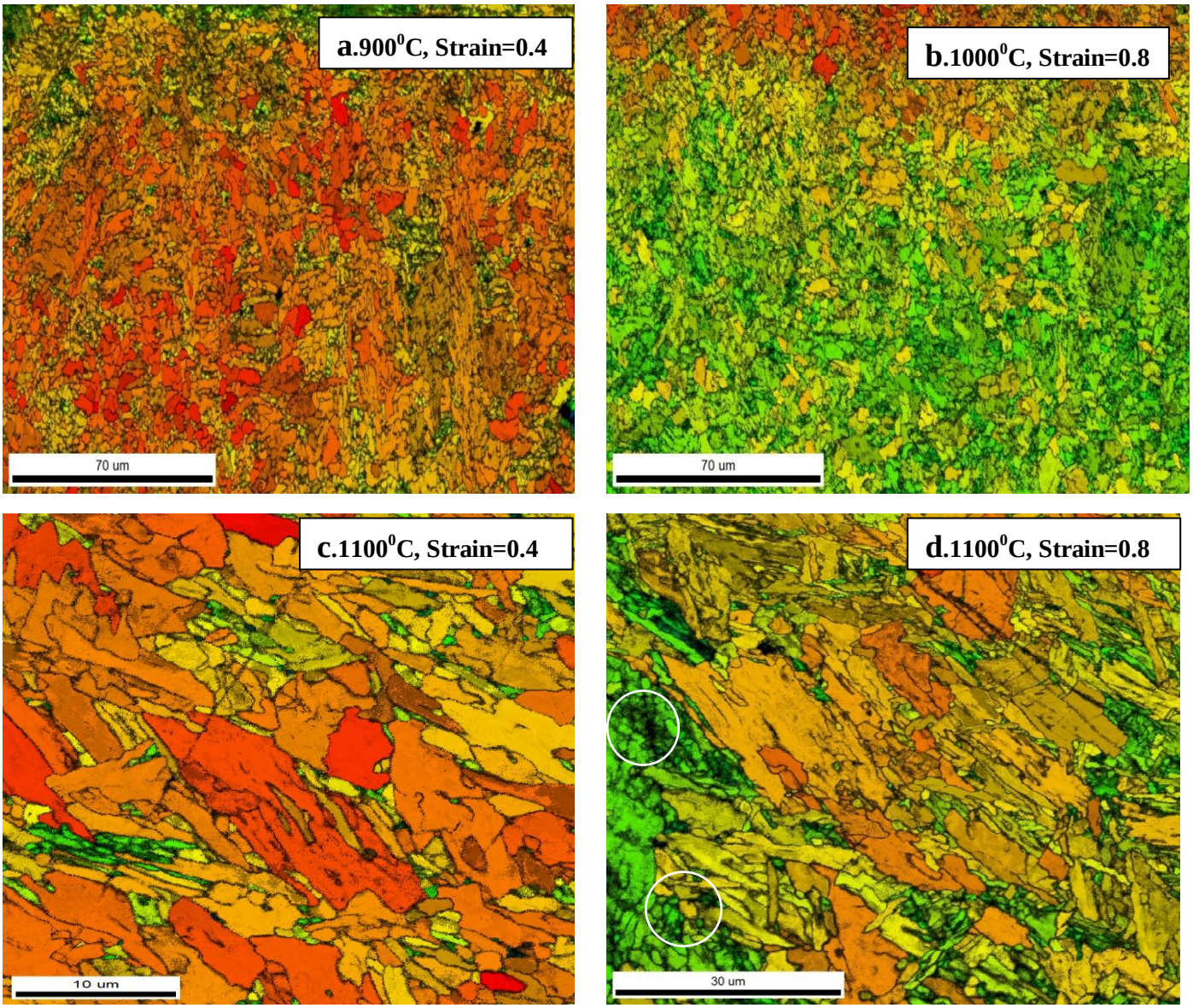

Figure 4.15 CI Average IQ colour coded maps for the selected samples deformed temperature of 900^{0}C (0.8 strain), 1000^{0}C (0.8 strain) and 1100^{0}C (0.4 and 0.8 strain) - white circle indicates the smaller nuclei at grain interfaces.

The confidence index is a measure of the how unambiguously close the indexing of the kikuchi pattern with the standard computer generated pattern. This map revealed the presence of smaller sub grains, which were otherwise not visible in the other maps, and responsible for the variation of colour coding within a grain in the IPF maps. It is also interesting to see much finer grain sizes are visible even at large deformation temperature of 1100°C as shown in encircled region.

4.6 Micro hardness Observations

The micro hardness was performed on the deformed samples as the size of samples was small. The hardness of as received APIX60 plate was ~160 Hv. The hardness was performed for the samples deformed at different deformation temperature.

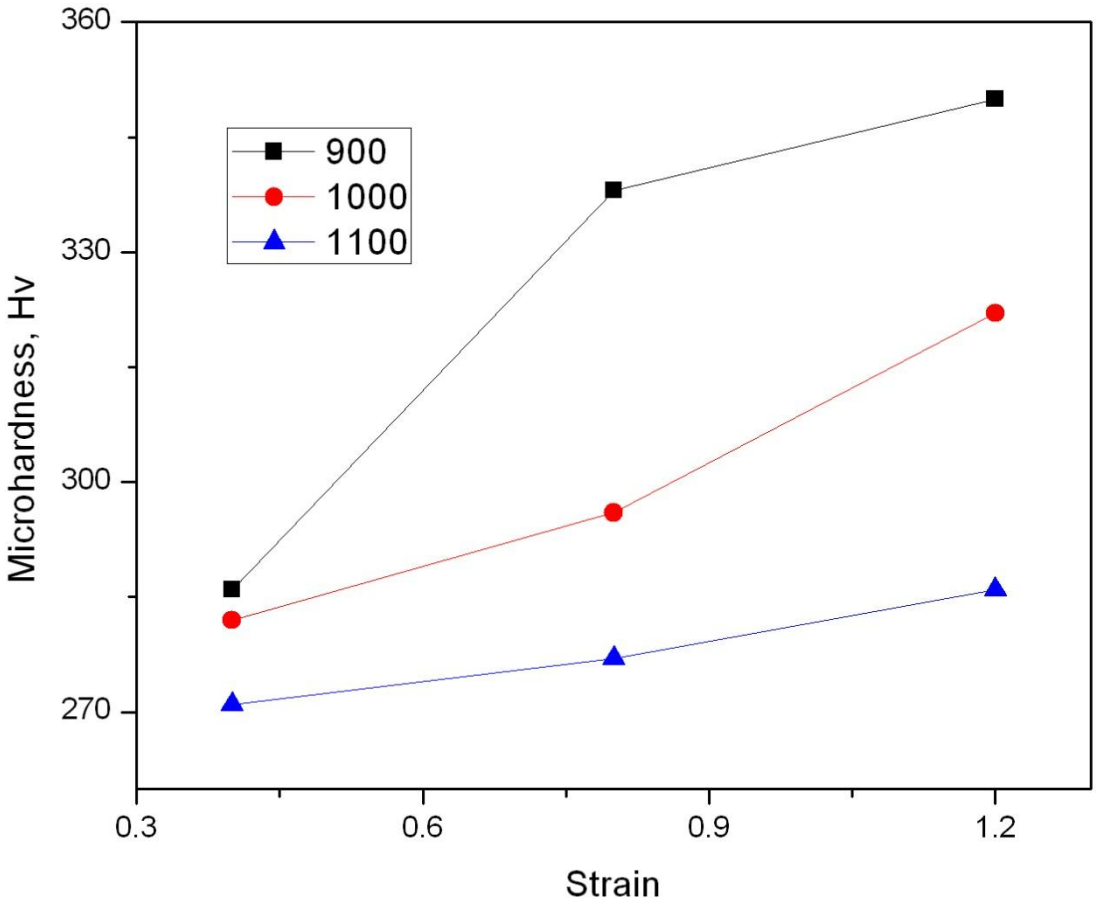

Figure 4.16 Micro hardness measurements for the samples cooled immediately after deformation.

The hardness results indicate that the samples deformed at lower temperature showed higher hardness values as compared to the sample deformed at higher temperatures. This is due to the fact that the softening effects are predominant in case of samples deformed at 1100°C and while acicular ferrite with fine grained structure is responsible for higher hardness values of above 300Hv. It is interesting that the improvement in strength values by grain refinement is more viable for these kinds of steels as compared to phase hardening (martensite formation) as the carbon content values are lower. There is increase in hardness with respect to increase in strain, the slope of hardness curves decreases with increase in deformation temperatures due to softening effects.

CHAPTER NO: 05

CONCLUSION

The objective of this project is to obtain ferrite grain refinement in X-60 grade pipeline steel by displacive transformed micro structural constituents like e.g. acicular ferrite, bainite, martensite/austenite etc instead of diffusive transformation products like pearlite and allotriomorphic ferrite. The present work, therefore aimed at studying the process parameters on the micro structural features, recrystallisation behaviour and mechanical properties obtained thereof for API X60 grade steel composition. This was done to assess the possibility of achieving properties commensurate with higher grades of API steel using the same composition.

The salient points of this investigation can be concluded here which are as:

1. From, the different order of stress-strain curve, It is possible to obtain the value of peak stress and critical stress and it corresponding strain value. As we know that, the formation of peak in the flow curve is the indication of onset of DRX (dynamic rerystallisation) and occurred at high temperature at 1100^0C and at a low strain value of ~0.4 for the given APIX60 grade steel.

2. From, the first order of stress –strain curve, It is possible to obtain the value of σ_{sat} which is used for calculating the volume of recrystallised fraction of material at different deformation temperature. It is observed that the volume of recrystallised fraction was ~ 0.5 at highest deformation temperature of 1100°C and low fraction of < 0.1 at a lower deformation temperature of 1000°C.

3. In the optical investigation, the microstructural combination of predominantly acicular ferrite along with some regions of bainitic laths was observed for sample processed at 900°C, while the sample deformed at 1000°C shows larger grain structure with more bainitic lath type regions and acicular ferrite. The samples deformed at 1100^0C shows very large size of some bainitic laths and martensite grains. There is effect of strain level on refinement of grain sizes for samples deformed at 900^0C and 1000^0C and there is no refinement of grain for samples processed at 1100^0C.

5. From SEM with EDS analysis, it appears to be the intragranular nucleation of acicular ferrite plates on the Ca-modified MnS inclusions. The formation of acicular ferrite is mainly occur at low temperature deformation such as 900^0C,which can easily seen from figure(4.9) of SEM micrographs, which is far below than Tnr and when the deformation occur far below than T_{nr}(non-recrystallisation Temperature) then as a result the ratio of grain boundary surface area to grain volume is increase, which provides more nucleation sites for ferrite transformation and also precipitation of Nb at large amount which can also act as favourable environment for the nucleation of acicular ferrite. The grain sizes are finer at low temperature due to absence of softening effect as observed from the flow curves. On the other hand, large under cooling at high temperature which cause formation of coarse grained martensite.

6. From the EBSD-OIM analysis, it is interesting to note that fraction of ~60^0 misorientation high angle boundaries increased with the increase in deformation temperature. However, the fraction of high angle

grain boundaries is highest at lowest temperature deformation such as 900^0C which indicates the formation of acicular ferrite is predominant at this deformation temperature. The inverse pole figure map indicates the grain orientation on the particular rolling plane. It is observed that the presence of smaller grains at the interface between large grains was observed to be of similar orientation for samples deformed at 900^0C, and to be of different orientation for samples processed at 1100^0C. This confirms that DRX has occurred at 1100^0C as predicted from the analysis of flow curves.

11. From the micro hardness results, it is observed that the sample which was deformed to ~0.8 true strain at lowest temperature of 900°C showed the hardness values of ~340 Hv while the other samples deformed at 1000°C and 1100°C showed hardness values much lower than 300Hv. As a result, it indicates the formation of harder fine grained acicular ferrite microstructure at lower temperature and it offers good combination of toughness and strength. It is also to be noted that the hardness for the processed samples are much higher than the as received sample.

REFERENCE

[1].Xiaoyong Zhang, Huilin Gao, Xueqin Zhang, Yan Yang, Materials Science and Engineering A 531 (2012) p. 84.

[2]. www.google.co.in/search?q=pipeline+distribution&newwindow.

[3].H Hara and M Kobayashi, Mitsubishi Motors Corporation, Material Engineering Division, Institute of metals vanadium award paper, (1987) p. 5 (http://vanitec.org/wp-content/uploads/2011/09/1987-The-Use-of-Hot-Forged-Microalloyed-Steels-in-Automobile-Components..pdf).

[4].M. Olasolo, P. Uranga, J. M. Rodriguez-Ibabe, B. Lopez, Material science and Engineering A 528 (2011) p. 2559.

[5]. Bert Verlinden,Indradev Samajdar,Roger D.Doherty,Thermo mechanical processing of metallic materials page 3.

[6]. S. V. Subramanian, G. Zhu, H. S. Zurob, G. R. Purdy, G. C. Weatherly, J. Patel, R. Kasper, Process modelling of micro alloyed steel . http://citeseerx.ist.psu.edu/viewdoc/summary?doi=10.1.1.136.995.

[7]. Dr.Ing Hans-Georg.Hillenbrand,Dr.Ing-Mechanical Gras and Dr.Ing Christoph Kalwa.Development and production of high strength pipeline steel.

[8]. J.Y.Koo,M.J.Luton,M.V.Bangan,R.A.Petkovi.Metallurgical Design of ultra Strength steel for Gas pipeline.

[9]. Specification for line pipe, ISO 3183:2007 (modified),petroleum and natural gas industries-steel pipe for pipeline transportation system, ANSI/API specification 5L, forty-fourth edition, oct.1, 2007.

[10].H Hara and M Kobayashi, Mitsubishi Motors Corporation, Material Engineering Division, Institute of metals vanadium award paper, (1987) p. 5 (http://vanitec.org/wp-content/uploads/2011/09/1987-The-Use-of-Hot-Forged-Microalloyed-Steels-in-Automobile-Components..pdf).

[11]. M. Olasolo, P. Uranga, J. M. Rodriguez-Ibabe, B. Lopez, Material science and Engineering A 528 (2011) p. 2559.

[12].P. D. Hodgson, S. H. Zahiri, J .J .Whale, ISIJ International, 44 (2004) p. 1224.

[13]. Ivani De S. Bott, Luis F. G. De Souza, Jose C.G. Teixeira, Paulo R.Rios, Metallurgical and Materials Transactions A 36A (2005) p. 443.

[14].Tamehiro, H., Asahi, H., Hara, T., Terada, Y., United States Patent 6264760, (1999).

[15]. Tamehiro, H., Asahi, H., Hara, T., Terada, Y., United States Patent 6264760, (1999)

[16].Liessem, A., Knauf, G., Zimmermann, S., Strain Based Design - What the Contribution of a Pipe Manufacturer Can Be, ISOPE 2007-SBD14 (2007) p. 1.

[17].Vervynckt, S., Control of the Non-recrystallization Temperature in High Strength Low Alloy (HSLA) Steels, PhD Thesis, Ghent University, 2010.

[18].Ya-bin Cao, Fu-ren Xiao, Gui-ying Qiao, Xiao-bing Zhang, Bo Liao, Material science and engineering A 530 (2011) p. 277.

[19].Klaus Hulka, J. M. Gray, High temperature processing of line pipe steels, www.cbmm.com.br/portug/sources/techlib/science/table./033.pdf

[20].Michael Korchynsky, A new role for microalloyed steels- adding economic value, Consultant in Metallurgy, U. S. Vanadium Corporation, A subsidiary of strategic minerals corporation, Pittsburgh, Pennsylvania, http://vanitec.org/wp-content/uploads/2011/09/A-New-Role-for-Microalloyed-Steels-Adding-Economic-Value.pdf.

[21].Junhua Kong, Lin Zheng, Lixin Wu, Xiaoguo Liu, Liwei Li, Mechanical properties and microstructure of X80 hot-rolled steel strip for the second west-east gas pipeline, Int. Conf. on Advanced Steels (ICAS 2010), Guilin city, Guangxi, China, (2010) p. 333.

[22]. G. R. Purdy, C. R. Hutchinson and Y. Brechet, ISIJ International, 45 (2005) p. 713.

[23]. Yoshi Terada, Hiroshi Tamehira, Mitsugu Yamashita, Naoshi Ayukawa, Takuya Hara, Nippa steel technical report no.72 January 1997

[24]. Hitoshi Asahi, Akira Yagi and Masakatsu Ueno, Metallurgical and Materials Transactions A 29A (1998) p.1375.

[25].O. A. Sofrygina, S. Yu. Zhukova, S. M. Bityukov, I. Yu. Pyshmintsev, Economical steels for the manufacturing of high-strength oil pipe (according to the API Spec5CT standard), ISSN 0967-0912, Steel in Translation 40 (2010) p.616.

[26].G. Zhu, S. V. Subramanian, Material science and engineering A 426 (2006) p. 235.

[27]. Z. Q. Sun, W. Y. Yang, J.J Qi, Mater. Sci. Forum 475-479 (2005) p.49.

[28].E. V. Konopleva ,H. J. McQeen, V. M. Khlestov, Proceeding of the thermomechanical Processing of steels, London, UK, May 24-26 (2000) p.287.

[29].S. Vervynckt, Control of the Non-recrystallization Temperature in High Strength Low Alloy (HSLA) Steels, PhD Thesis, Ghent University, 2010

[30].H. Asahi, Development of Ultra-high-strength Pipeline, X120, Nippon Steel Technical Report 90 (2004) p. 82.

[31].A. Liessem, C. Kalwa, C. Stallybrass, S. Mannesmann & GmbH, Technological Solutions for High Strength, Europipe Technical Publications, 2008.

[32]. https://www.google.co.in/search?q=pearlite%2Bbainite+microstructure&newwindow.

[33]. R.W.k.Honeycombe and H.K.D.H.Bhadeshia, Publishesd by Elsevier ltd, steel page no 155.

[34]. Alberto Moreira Jorge Junior, Luiz Henrique Guedes, Oscar Balancin, Journal of Materials Research and Technology 1 (2012) p. 141.

[35]. G R Speich , V A Demarest , R L Miller, Metal. Trans A 12 (1981) p. 1419.

[36]. M A F Oliveira, A M Jorge Jr., O. Balancin, Scripta Mater 50 (2004) p. 1157.

[37]. S. Yue, J. J. Jonas, Materials Forum 14 (1990) p. 245.

[38]. J. H. Beynon, C. M. Sellars, ISIJ International 32 (1992) p. 359.

[39].R.L.Bondar,R.O.Adebanjo and S.S.Hansen, "Determination of the TR and Ar3 temperaturees fraom roll face measurements"in 37th Mechanical Working and steel Processing Confernce,1996,pp 743-757.

[40].S.Vernynckt,K Verbeken,B.Lopez and J.J.Joneas, "Morden HSLA steels and role of non-recrystallisation temperature," International Materials Reviews,vol 57,pp 187-207,2012.

[41].L.N.Pussegoda and J.J.Jonas "Comparsion of dynamic recrystallisation and conventional controlled rolling schedules by laboratory simulation,ISIJ International ,vol.31,pp 278-288,1991.

[42].S.Vervynckt,K.Verbeken,P.Thaibaux,M.Liebeherr,and Y.Houbaert, "Austenite recrystallisation-precipitation interaction in Nb microalloyed steel, "ISIJ Interational ,vol.49 pp 911-920,2009.

[43].D.Q.Bai,S.Yue ,W.P.Sun and J.J.Jonas, "Effect of deformation parameters on the non-recrystallisation temperature in Nb steels," "Metaullurgical transcation A,volume 24,pp 2151-2159.

[44].F.Flecther, "Meta-analysis of T_{nr} measurement, "Determine new empirical models based on compositions and strain" in Austenite Processing Symposuim (Internationa Company Presentation),2008,pp1-14.

[45].Ya-bin Cao,Fu-ren Xiao,Gui-ying Qiao,Xiao-bing Zhang,Bo Liao "Quntative research on effect of Nb on hot deformation behaviours of high Nb micro alloyed steel .

[46].L.J.Cuddy, "The effect of microalloy concentration the recrystallisation of autenite during hot deformation." In Thermo mechanical Processing of micro alloyed Austenite, 1982 pp-129-140.

[47]. http://en.wikipedia.org/wiki/Avrami_equation.

[48].Johan.J.Jones, Xavier Quelence, LanJiany, Etiemme Martin, the Avrami-kinectics of dynamic recrystallisation.

[49].Poliak EI, Jonas.J.J,Acta Mater 1996;44 127.

[50].T.Gladman,The physical Metallurgy of microalloyed Steels,2nd London,Maney Publishing 2002,p563.

[51].W.F.Haeford, R.M.Caddell, Metal Forming, Mechanics and Metallurgical, 3rd, New York Cambridge University Press 2007,p372.

[52].G.E.Dieter, Mechanical Metallurgical 3rd vol.45 McGraw-Hill London 1986.

[53].E.P.Degarmo,J.T.Black, and R.A.Kohser,Material and Process in Manufacturing,9th ed.Hoboken,NJ. Johwiley and Sons.Inc, 2003.p 1154.

[55].V.B.Ginzburg, Metallurgical Design of Flat Rolled Steels, New York Marcel Dekkar, 2004, p: 726.

[56]. http://en.wikipedia.org/wiki/Dilatometer.

[57].http://thermophysical.tainstruments.com/instruments/dilatometers/dil-805ad-quenching-and-deformation-dilatometer.

[58]. http://thermophysical.tainstruments.com/instruments/dilatometers/?gclid=CLWshPLaq74CFdckvQodJiQAcQ.

[59]. http://gleeble.com/index.php/products/gleeble-3800.html.

[60] http://civil.eng.buffalo.edu/cie616/2-LECTURES/Lecture%204a%20-%20material20%hardness.

[61]. http://en.wikipedia.org/wiki/Scanning_electron_microscope.

[62]. /www.google.co.in/search?newwindow=1&site=webhp&q=ebsd+image&oq=ebsd+image

[63]. https://www.google.co.in/search?q=kikuchi+pattern+image&newwindo.

[64]. Deardo AJ. Modern, Thermomechanical processing of microalloyed steel: A physical metallurgy perspective. Proc. Microalloying' 95 Conf., June 11–14, 1995. Pittsburgh, PA: The Iron and Steel Society (1995) p. 15.

[65]. P. Cizek, Transformation Behaviour & Microstructure of an API X80 Linepipe steel subjected to simulated thermomechanical processing, METAL 2001, Ostrava, Czech Republic (2001) p. 1.

[66]. R. D. K. Misra, G. C. Weatherly, J. E. Hartmann and A. J. Boucek, Material Science and Technology, 17 (2001) p. 1119.

[67]. Xu Wang, Fu-ren-Xiao, Yan-hong Fu, Xiao-wei Chen, Bo Liao, Materials Science and Engineering A, 530 (2011) pp. 539-547.

[68]. Adem Bakkaloglu, Materials Letters, 56 (2002) p.200.

[69]. N. D. Ryan, H. J. McQueen, Canadian Metallurgical Quarterly, 29 (1990) p. 147.

[70]. G. R. Stewart, J. J. Jonas, F. Montheillet, ISIJ International 44 (2004) p. 1581.

[71]. E.I. Poliak and J. J. Jonas, Acta Materialia 44 (1996) p. 127.

[72]. E.I. Poliak and J. J. Jonas, ISIJ International 43 (2003) p. 692.

[73]. E. I. Poliak, J. J. Jonas, ISIJ International 43 (2003) p. 684.

[73].A Najafizadeh, J. J. Jonas, ISIJ International, 46 (2006) p. 1679.

[74]. A.S. Taylor and P.D. Hodgson, Materials Science and Engineering A 528 (2011) p. 3310.

[75].E. I. Poliak, J. J. Jonas, ISIJ International, 43 (2003) p. 684.